Title
NEUTRON STARS ARE GIANT HYPERNUCLEI?

Author
Glendenning, N.K.

Publication Date
1984-03-01

LBL-15976 c.2
Preprint

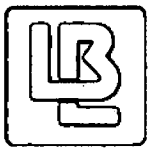

Lawrence Berkeley Laboratory
UNIVERSITY OF CALIFORNIA

Submitted to the Astrophysical Journal

NEUTRON STARS ARE GIANT HYPERNUCLEI?

N.K. Glendenning

March 1984

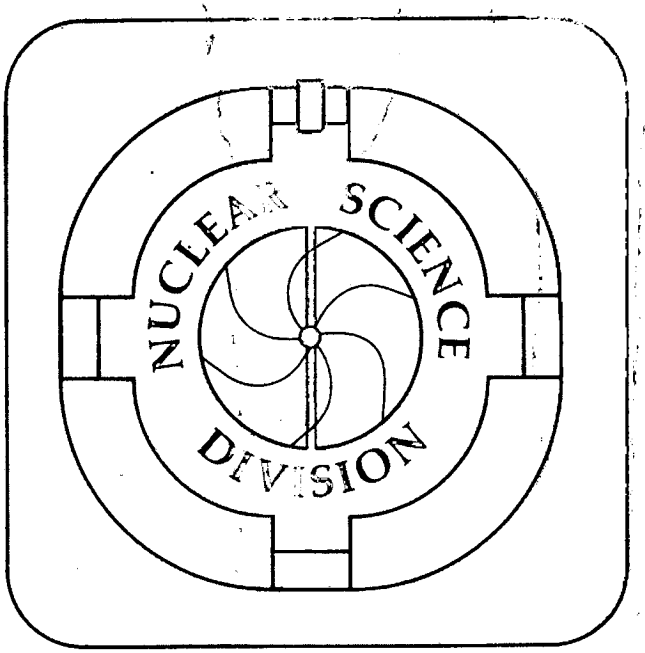

Prepared for the U.S. Department of Energy under Contract DE-AC03-76SF00098

DISCLAIMER

LBL-15976

Neutron Stars are Giant Hypernuclei?

Norman K. Glendenning

Nuclear Science Division
Lawrence Berkeley Laboratory
Unversity of California
Berkeley, CA 94720

Abstract

Neutron stars are studied in the framework of Lagrangian field theory of interacting nucleons, hyperons and mesons, which is solved in the mean field approximation. The theory is constrained to account for the four bulk properties of nuclear matter, the saturation binding and density, compressibility and charge symmetry energy. The cores of the heavier neutron stars are found to be dominated by hyperons and the total hyperon population for such stars is 15-20%, depending on whether pions condense or not. The rho meson, which contributes to the isospin symmetry energy, has an important influence on the baryon populations. Lepton populations are strongly suppressed and charge neutrality is achieved among the hadrons. A possible consequence for the decay time of the magnetic field of pulsars and hence for their active lifetime is mentioned.

This work was supported by the Director, Office of Energy Research, Division of Nuclear Physics of the Office of High Energy and Nuclear Physics of the U.S. Department of Energy under Contract DE-AC03-76SF00098.

Neutron Stars are Giant Hypernuclei?

Norman K. Glendenning

Nuclear Science Division
Lawrence Berkeley Laboratory
University of California
Berkeley, CA 94720

I. Introduction

Although a fundamental theory of matter would be based (presumably) on quarks and gluons, in the density range of neutron stars the elementary constituents are most likely confined in hadrons. In this case an *effective* Lagrangian field theory can be employed that treats the hadrons as the interacting fields. This is analogous to discussing ordinary matter in terms of atoms and molecules instead of neutrons, protons, and electrons (or quarks, gluons, and electrons).

In the last few years such an approach based on a relativistic field theory involving interacting nucleons and a scalar and vector meson, and solved in the mean field approximation, has had remarkable success in describing nuclei. The coupling constants of the theory are regarded as adjustable parameters that are fixed by demanding that the theory account for the saturation density and binding[1,2] and the compressibility[3,4] of symmetric nuclear matter. Once having determined the parameters in this way, the theory has been shown to account for a large number of single-particle properties of finite nuclei.[5,6] In addition to properties of the normal ground state, the pion condensed state has also been investigated in extensions of the theory.[7,8,9] However this state is expected to lie at densities above the normal density and its existence has so far not been verified.

In this paper we build upon the above approach.[10] For neutron stars the charge symmetry energy must be of vital importance, so it is added to the list of bulk nuclear properties that the theory must account for. Moreover at high density, additional baryons besides the nucleons may be present, including the Δ and the hyperons, Λ, Σ, . . .and they too can be incorporated as in our earlier work.[11]. Within such a relativistic field theory of interacting nucleons, isobars, hyperons and mesons we investigate a number of properties of neutron stars, and suggest a possible consequence of the existence of hyperon populations.

There have been earlier discussions than this one concerning hyperons in neutron stars. The very early discussion of Ambartsumyan and Saakyan[12] based on Fermi gases makes a very plausible case for the existence of a hyperon charge on neutron stars. Later calculations included effects of nuclear forces in the Schroedinger theory.[13-16] The main focus of the traditional Breuckner-Bethe approach to the nuclear many-body problem has been on the saturation density and binding. So far there is no general agreement on convergence of the theory to the empirical values. Consequently the symmetry energy and nuclear compressibility are also as yet uncontrolled in the traditional approach. The absence of a control on the symmetry energy is very serious for neutron stars and accounts for some of the major differences between our results and earlier ones.[13-17]

In our theory we retain relativistic covariance. Consequently our equation of state automatically respects the causality limit, $p < \rho$. This is sometimes a problem with the Schoedinger theory.

In the following sections the general principles of chemical equilibrium for a system that has lived a long time with respect to some elementary processes and a short time with respect to others is discussed. We describe the Lagrangian, discuss its completeness and the related question of phase transitions, derive the self-consistency conditions for the mean fields, and

show how to calculate the baryon currents, which are sources of various mesons. Then numerical solutions of the theory are presented. A number of features are investigated including the role of the rho-meson (isospin symmetry energy), the hyperons, and a pion condensate. It is found that the ground state of dense, charge-neutral matter develops large populations of hyperons as the density of matter approaches that which is typical of the center of heavier neutron stars. The development of such populations in a star that originally contained no strange particles is not in violation of the fundamental laws of elementary processes but a consequence of them. The kaons, produced in association with hyperons, decay on a time scale $\sim 10^{-10}$ sec with the eventual leakage of photons and neutrinos, thus lowering the energy of the star. Consequently, the strange baryons become Pauli blocked from decaying back to nucleons. In this way the strangeness quantum number evolves until the neutron star becomes cold. We calculate density profiles of the various baryons in typical neutron stars and check the populations for uncertainties in the theory. The hyperons are found to be the dominant population in the cores of the heavier neutron stars and are about 15 to 20 percent of the total baryon population of such stars. It is also found that charge neutrality is achieved through the cancellation of charges on *massive* particles. The electron and muon populations are quenched by hyperons and pions. The possible consequences for the electrical conductivity (and hence the lifetime of the magnetic field of pulsars) is suggested.

II. Chemical Equilibrium in a Star

To understand the nature of chemical equilibrium in a star it is useful to note that they evolve and that a cold neutron star is a possible *ground* state configuration. Many different reactions can occur during the evolution. Toward the end of the evolutionary phase, reactions between hadrons occur. Any photons or neutrinos produced in these reactions can eventually leak out, thus lowering the star's energy. Certain quantum numbers are conserved absolutely or on a time scale long compared to the evolutionary period or the period over which observations are made on the star. Others are violated by weak and electromagnetic interactions on a short time scale. Therefore, the ground state of a star is to be found as a problem of chemical equilibrium subjected only to the constraints of baryon and electric charge conservation. The strangeness quantum number, for example, exerts no constraint on the evolution of the star whatsoever. Thus, when the Fermi momentum of nucleons is sufficiently high, reactions such as

$$N + N \rightarrow N + \Lambda + K \tag{1}$$

become possible. The associated kaon is free to decay (unless driven by a phase transition as discussed later). For example

$$K^0 \rightarrow 2\gamma \tag{2}$$

$$K^- \rightarrow \mu^- + \nu$$

$$\mu^- + K^+ \rightarrow \mu^- + \mu^+ + \nu \rightarrow 2\gamma + \nu$$

The star's energy is lowered through the leakage of the photons and neutrinos. Consequently, the Λ becomes Pauli blocked, and a net strangeness can evolve for sufficiently dense neutron stars. Other hyperons are populated as the density of nucleons increases.

Of course, solving a problem of chemical equilibrium does not require that individual reactions be studied such as the examples cited above. It requires only the recognition of which attributes are conserved by the system. It is the electro-weak interactions that determine which attributes are not conserved. To high precision, they play no further role in the determination of the ground state energy. The energy and particle populations are determined by the strong interactions, the baryon masses, charges, and isospin projections, subject only to the constraints

imposed by the long-lived attributes. These being baryon number and electric charge, all particle chemical potentials can be written in terms of the two independent chemical potentials μ_n and μ_e for baryon number and (negative) electric charge.

For example, at densities in the vicinity of nuclear matter density, charge neutral matter is almost pure in neutrons, but must have a small admixture of protons with an equal number of electrons to establish equilibrium with respect to $n \longleftrightarrow p + e^- + \bar{\nu}_e$. For a cold star, neutrinos and photons escape and equilibrium is established when the Fermions occupy their lowest energy states up to energies that satisfy the balance

$$\mu_p = \mu_n - \mu_e \tag{3}$$

As the neutron density increases, so does that of electrons. Eventually μ_e reaches a value equal to the muon mass. Thereafter it too will be populated and equilibrium with respect to $e^- \longleftrightarrow \mu^- + \nu_e + \bar{\nu}_\mu$ is assured when $\mu_\mu = \mu_e$. The weak and electromagnetic decays (2) together with the vanishing populations of neutrinos and photons imply that

$$\mu_{K^0} = 0, \quad \mu_{K^-} = \mu_e, \quad \mu_{K^+} = -\mu_e \tag{4}$$

while equilibrium with respect to (1) yields

$$\mu_\Lambda = \mu_n \ . \tag{5}$$

In general for an arbitrary particle , chemical equilibrium in a star in which baryon number and electric charge are conserved are expressed by

$$\mu = q_b \mu_n - q_e \mu_e \tag{6}$$

where q_b and q_e are the baryon and electric charge of the particle in question. This particle will be populated when μ exceeds its lowest eigenstate in the medium. In the absence of interactions, this will be its mass. Interactions will of course shift the threshold as we shall see explicitly in later sections.

III. The Relevant Hadronic Fields, Phase Transitions

In this section we will determine which are the relevant hadronic fields. The Lagrangian will consist of the free Lagrangians of leptons, baryons, and mesons, together with an interaction Lagrangian. The strong interaction Lagrangian is

$$\mathscr{L}_{\text{strong}} = \sum_B \mathscr{L}_B^0 + \sum_M \mathscr{L}_M^0 + \mathscr{L}_{\text{int}} \tag{7}$$

where B is summed over the baryons

$$B = n, p, \Lambda, \Sigma^{-,0,+}, \ \Xi^{-,0}, \Delta^{-,0,+,++}, \ldots \tag{8}$$

Their quantum numbers and masses are listed in Table I. We shall find that no others are populated up to baryon densities substantially higher than the 1.2 fm^{-3} limit that we place on our discussion. M is summed over mesons of various quantum numbers. Table II lists some of the mesons, their quantum numbers, and typical interaction Lagrangians, which, of course, must be Lorentz scalars. It will become apparent that the theory depends on the meson masses and coupling constants only through the ratios g/m, and these ratios are determined for those mesons that contribute to the normal state of matter by demanding that the theory account correctly for the four bulk properties mentioned in the introduction.

The Euler-Lagrange equations for the ground state expectation values of the meson fields are,

$$
\begin{aligned}
(\Box + m_\sigma^2) <\sigma> &= \sum_B g_{\sigma B} <\bar{B}B> \\
(\Box + m_\omega^2) <\omega_\mu> - \partial_\mu \partial^\nu <\omega_\nu> &= \sum_B g_{\omega B} <\bar{B}\, \gamma_\mu\, B> \\
&\vdots \\
(\Box + m_K^2) <K> &= g_K <\bar{\Lambda}\gamma_5 N> + \cdots \\
&\vdots
\end{aligned}
\tag{9}
$$

The kaon has both neutral and charged states and the appropriate baryons are understood to appear on the right. The sources in these field equations are the ground state expectation values of the baryon currents that appear in the interaction Lagrangian of Table II.

Certain of these sources have familiar meanings. For example, the baryon number density is

$$n = \sum_B <\bar{B}\,\gamma_0\, B> = \sum_B <B^\dagger\, B> \tag{10}$$

This density drives the ω-meson. The 3-component of the isospin density

$$<I_3> = \frac{1}{2}\sum_B <\bar{B}\,\gamma_0\,\tau_3\, B> \tag{11}$$

drives the neutral ρ-meson, while the scalar density, $<\bar{B}B>$ drives the σ-meson. However, not all source currents on the right sides of the field equations (9) will be simultaneously finite. We define the *normal* state of infinite matter to have the following characteristics: it is uniform and isotropic, and, in addition, the baryon eigenstates in the medium carry the same quantum numbers as they do in vacuum. Then pseudo-scalar and pseudo-vector currents vanish in the normal state as well as the nondiagonal currents that are sources of the charged rhos and the kaons. The $\bar{\Lambda}\gamma_5 N$ current, for example, changes the number of nonstrange and strange baryons each by one unit and therefore has vanishing expectation value in the normal ground state. Consequently such mesons, π, $\rho^\pm$, K, K^* as would be driven by these currents satisfy the field equation for free particles in the normal ground state, and therefore *they can decay freely*. The star's energy will be lowered in the subsequent leakage of any neutrinos and photons produced in the decays.

We come now to the question of phase transitions by which we mean a change in the character of the ground state of the system such that additional source currents besides the three mentioned above acquire a finite value. The meson coupled to such a source current then ceases to be free and is driven to have a finite amplitude. The pion condensate has been extensively studied.[18,7-9]. The repulsive s-wave π-N interaction inhibits condensation by raising the effective mass of the pion in matter. Consequently condensation, if it occurs, will do so by virtue of the attractive p-wave interaction. For this reason the pion condensed phase has finite wave vector $\underline{k}$ and corresponds to a phase in which the isotropy of matter is broken. We now consider the plausibility of additional condensates.

Consider the kaon as a general example of a meson whose source current vanishes in the normal state. Rewrite the field equation for the Fourier components as

$$[-k_\mu^2 + m_K^2 + \Pi_K(k_0,\underset{\sim}{k})] <K> = 0 \tag{12}$$

where $k_\mu^2 = k_0^2 - \underset{\sim}{k}^2$. Consider this at the threshold of a possible phase transition. In this case Π_K is known as the polarization operator or self-energy and can be written as

$$\Pi_K = - \lim_{<K>\to 0} \frac{<J>}{<K>} \tag{13}$$

where J is the source current on the right side of (9). The nonrelativistic form of (13) is the Lindhardt function. The essential point, however, is that (12) implies that the condition for nonvanishing <K> is

$$-k_0^2 + \underset{\sim}{k}^2 + m_K^2 + \Pi_K(k_0,\underset{\sim}{k}) = 0 \tag{14}$$

The threshold baryon density for the charged K^- condensate is that density for which this equation first has a solution for real $\underset{\sim}{k}$ and for $k_0 = \mu_e$, the electron chemical potential. A similar equation holds for the π^-. We can now discuss the plausibility of phase transitions in terms of the pion condensate. First note that from nuclear matter density, the electron chemical potential, $\mu_e = \mu_n - \mu_p$, is an increasing function of density until it attains a value on the order of the pion mass. At that point negative pions will condense, and being bosons they can condense in the same energy state. Therefore, μ_e will tend to saturate. The saturation point would be precisely m_π if the pion did not interact with other hadrons. In the presence of interactions the discussion is more complicated. The s-wave repulsion in the π-N interaction produces a positive polarization operator and tends to inhibit condensation. In this event μ_e would not saturate at m_π but at some larger value or not at all. The p-wave interaction, on the other hand, is attractive but requires that the pion have non-zero wave number, k. Actual calculations of pion condensation in neutron star matter indicate that a condensate is expected with k $\sim$ 1.5 fm^{-1} and that μ_e saturates at $\sim$177 MeV.[9] The consequence of the saturation of μ_e near the pion mass, is that the pion forecloses the possibility of other types of phase transitions. Since $k_0 = \mu_{K^-} = \mu_e$ in (14) is bounded from above by the pion, the polarization operator Π for the K^- would have to be very large and attractive so as to overcome its large mass in order that (14) be satisfied. However, the experimental evidence on kaon-nucleon interactions suggests that they are weaker than pion interactions. In this case the kaon cannot condense. It is even less plausible that the K^* would condense.

We have focused the above discussion on negatively charged mesons since their chemical potential, μ, equals that of the electron, which in a neutron star is positive, $\mu_e = \mu_n - \mu_p$. The threshold condition for a free particle is obviously $\mu \geq \sqrt{k^2+m^2}$ which cannot be satisfied for a neutral (μ=0) or positively charged (μ=$-\mu_e$) free meson. These conclusions remain valid for interactions with the medium, so long as they are not strongly attractive. So the above discussion is certainly adequate for all charged states of the kaon. The π-N attractive interaction in the p-wave can modify the discussion for pions because of the structure of $\Pi(k_0, \underset{\sim}{k})$ in such a case. It is possible that the π_s^+ spin-isospin sound mode discussed in reviews by Migdal and by Baym could be lower than the π^-.[18] However taking into account s and p-wave interactions and coupling to the isobars we find for our quasiparticle spectrum (case 5 discussed later is the appropriate one) that the π^- remains lower than π_s^+.

Our conclusion, therefore, is that the only meson that can condense in neutron stars is the π^-, other than those that are driven by finite baryon source currents in the normal state (the σ, ω, ρ°). The complexity of the interaction Lagrangian, relevant to ground state properties of charge neutral matter, is thus strongly limited by the pion.

IV. Lagrangian and Field Equations

Following from the discussion of the preceding section, the Lagrangian from which we can derive the equation of state of neutron star matter can be written for the hadronic phase as

$$\mathscr{L} = \sum_B \bar{B}(i\gamma_\mu \partial^\mu - m_B + g_{\sigma B}\,\sigma - g_{\omega B}\,\gamma_\mu\,\omega^\mu)\,B$$

$$- g_\rho\,\rho_{\mu 3}\,J_3^\mu + \mathscr{L}_\sigma^0 + \mathscr{L}_\omega^0 + \mathscr{L}_\rho^0 + \mathscr{L}_\pi^0 - U(\sigma) + \sum_{\lambda=e^-,\mu^-} \bar{\Psi}_\lambda(i\gamma_\mu\,\partial^\mu - m_\lambda)\Psi_\lambda \qquad (15)$$

Here B denotes a Dirac spinor for the baryon B, and $\bar{B} = B^\dagger\,\gamma_0$.[19] The pion hadronic interactions will be ignored. As we will see later, this approximation will provide a conservative estimate of hyperon populations. Of the charged states of the ρ meson, only the neutral is kept, which is denoted by the subscript 3 corresponding to its isospin projection. The others are rejected by virtue of the discussion of section III since their sources vanish in normal matter.

In the above equation J_3^μ is the 3-isospin component of the isospin current

$$\underset{\sim}{J}^\mu = \frac{1}{2}\sum_B \bar{B}\,\gamma^\mu\,\underset{\sim}{\tau}\,B + \underset{\sim}{\pi} \times \frac{\partial\mathscr{L}}{\partial(\partial_\mu\,\underset{\sim}{\pi})} + \underset{\sim}{\rho}_\nu \times \frac{\partial\mathscr{L}}{\partial\,(\partial_\mu\,\underset{\sim}{\rho}_\nu)} \qquad (16)$$

The coupling of the neutral rho meson to the isospin density provides a driving force to isospin symmetry and, in normal nuclei, is responsible for the symmetry energy. (The last two terms in (16) can be dropped because we shall introduce pions only as free particles and because the the rho field is space-time independent in infinite matter.)

The potential $U(\sigma)$ represents self-interactions of the scalar field[3] and is important in reducing the unrealistically large value of the nuclear compressibility of the Walecka model.[2] Its specific form is

$$U(\sigma) = [bm_N + c(g_\sigma\sigma)]\,(g_\sigma\sigma)^3 \qquad (17)$$

The mean field approximation consists of replacing all baryon currents in the Euler-Lagrange equations that follow from (15) by their ground state expectation values. The baryon ground state consists of a degenerate Hartree state constructed from solutions of the field equations for the baryons in which meson fields are replaced by their mean values. The resulting equations are coupled nonlinear equations that are to be solved for the self-consistent values of the mean fields. Particle populations are to satisfy the conditions of chemical equilibrium and, in the case of a star, charge neutrality.

The Dirac equations for the baryons that follow from (15) are

$$[\not{p} - g_{\omega B}\,\not{\omega} - \frac{1}{2}g_{\rho B}\,\tau_3\,\not{\rho}_3 - (m_B - g_{\sigma B}\,\sigma)]\,B = 0 \qquad (18)$$

where $\not{p} = \gamma_\mu p^\mu$ and ω, ρ, σ now denote ground state expectation values. The spin-degenerate eigenvalue spectrum for the baryons follows upon rationalizing the Dirac operator. We find

$$\epsilon_B(\underset{\sim}{p}) = g_{\omega B}\,\underset{\sim}{\omega}_0 + g_{\rho B}\,\rho_{03}\,I_{3B} \pm E_B(\underset{\sim}{p}) \qquad (19)$$

$$E_B(\underset{\sim}{p}) = \left[(\underset{\sim}{p} - g_{\omega B}\,\underset{\sim}{\omega} - g_{\rho B}\,I_{3B}\,\rho_3)^2 + (m_B - g_{\sigma B}\,\sigma)^2\right]^{1/2} \qquad (20)$$

where I_{3B} denotes the 3-component of isospin of the baryon B and m_B is its mass. The $\pm$ sign in (19) corresponds respectively to particles and holes. Table I lists all of the baryons that are populated up to densities of 1.2 fm^{-3}. The field equations that are satisfied by the mean meson fields are

$$m_\sigma^2\,\sigma = -\frac{dU}{d\sigma} + \sum_B g_{\sigma B} <\bar{B}\,B> \tag{21}$$

$$m_\omega^2\,\omega_\mu = \sum_B g_{\omega B} <\bar{B}\,\gamma_\mu\,B> \tag{22}$$

$$m_\rho^2\,\rho_{\mu 3} = \frac{1}{2}\sum_B g_{\rho B} <\bar{B}\,\gamma_\mu\,\tau_3\,B> = \sum_B g_{\rho B}\,I_{3B} <\bar{B}\,\gamma_\mu\,B> \tag{23}$$

These are all coupled through the baryon currents appearing in them because of (18). The total electric charge density is

$$Q = \sum_B q_B <B^\dagger B> - \left[\sum_\lambda \frac{k_\lambda^3}{3\pi^2} + n_\pi \Theta(\mu_\pi - m_\pi)\right] e \tag{24}$$

where q_B is the charge on baryon B, k_λ is the Fermi momentum of lepton λ, n_π is the π^- charge density, which is zero if $\mu_\pi = \mu_e < m_\pi$, and Θ is the step function that is unity for zero or positive argument and zero otherwise.

Chemical equilibrium is imposed through the chemical potentials and involves two independent potentials μ_n and μ_e corresponding to baryon and electric charge conservation as previously discussed. For baryon B the chemical potential is

$$\mu_B = \mu_n - q_B \mu_e \tag{25}$$

while for π^-, μ^-, and e^- the chemical potentials are

$$\mu_\pi = \mu_\mu = \mu_e \tag{26}$$

The Fermi momenta of the baryons, k_B, are the positive real solutions of

$$\mu_B = \epsilon_B(\underset{\sim}{k}_B) \tag{27}$$

and the remaining Fermi momenta are determined by

$$\left(k_e^2 + m_e^2\right)^{1/2} = \mu_e \tag{28}$$

$$\left(k_\mu^2 + m_\mu^2\right)^{1/2} = \mu_\mu = \mu_e \tag{29}$$

$$\left(k_\pi^2 + m_\pi^2\right)^{1/2} = \mu_\pi = \mu_e \tag{30}$$

when the solutions are real and otherwise zero.

The equations (21–30) provide a set of coupled transcendental relations defining the meson field amplitudes, Fermi momenta, and chemical potentials. We shall see in the next section that the space-like components of the $\rho_{\mu 3}$ and ω_μ fields vanish identically. The list of unknowns is therefore

$$\sigma,\ \omega_0,\ \rho_{03},\ \mu_n,\ \mu_e,\ k_e,\ k_\mu,\ k_\pi,\ k_p,\ k_n,\ k_\Lambda, \ldots k_\Xi, \ldots$$

of which there are (8 + N) where N is the number of baryon types included (Table I). Notice that the lowest energy state has $\mu_e \leqslant m_\pi$. When the equality holds then n_π replaces μ_e as an unknown, and its value is to be determined from (24). Of course in the ground state, the free

pions will condense in the zero momentum state.

V. Evaluation of the Source Currents

The source currents appearing in the field equations (21–23) are very easy to obtain in explicit form because we have an explicit expression for the Fermion eigenvalues (19). The Dirac Hamiltonian following from (18) is

$$H_B = \gamma_0 [\underset{\sim}{\gamma}\cdot\underset{\sim}{p} + g_{\omega B}\,\phi + \frac{1}{2} g_{\rho B}\,\tau_3\,\not{\rho} + m_B - g_{\sigma B}\,\sigma] \tag{31}$$

Notice that the eigenvalues (19–20) do not depend on the intrinsic spin of the baryon. Denote the z-component by μ. A single-particle state is then characterized by p and μ. Denote the creation operator for such a state by $a^\dagger_{p\mu}$. According to the definition of the ground state given in the previous section, the ground state expectation of any operator Γ is

$$<\Gamma> = \sum_B <B^\dagger \Gamma B> = \sum_B \sum_\mu \int \frac{d^3p}{(2\pi)^3} <B^\dagger \Gamma B>_{\underset{\sim}{p}\mu}\,\Theta_B \tag{32}$$

where

$$<B^\dagger \Gamma B>_{\underset{\sim}{p}\mu} = <0|\,a_{\underset{\sim}{p}\mu}\,B^\dagger \Gamma B\,a^\dagger_{\underset{\sim}{p}\mu}\,|0> \tag{33}$$

and $\Theta_B \equiv [\mu_B - \epsilon_B(p)]$ is the step function previously defined, which here is unity if $\epsilon_b(p)$ is equal to or less than the chemical potential μ_B. Take the expectation of H_B with respect to a single-particle state,

$$<B^\dagger H_B B>_{\underset{\sim}{p}\mu} = <0|\,a_{\underset{\sim}{p}\mu}\,B^\dagger H_B\,B\,a^\dagger_{\underset{\sim}{p}\mu}\,|0> = p_0 = \epsilon_B(\underset{\sim}{p}) \tag{34}$$

where $\epsilon_B(p)$, which is independent of μ, is given by (13). From this equation we can derive the relations that are needed to obtain explicit expressions for the source currents and number density.

To evaluate the source of the ω field, take a derivative of (34) with respect to p_i. The result is

$$<\bar{B}\,\gamma_i\,B>_{\underset{\sim}{p}\mu} = \frac{\partial \epsilon_B(\underset{\sim}{p})}{\partial p_i}\ . \tag{35}$$

Hence

$$<\bar{B}\,\gamma_i\,B> = (2J_B + 1)\int \frac{d^3p}{(2\pi)^3}\,\frac{\partial \epsilon_B(\underset{\sim}{p})}{\partial p_i}\,\Theta_B$$

$$= (2J_B + 1)\int \frac{dp_j dp_k}{(2\pi)^3} \int d\epsilon_B(p_j,p_k)\Theta_B = 0\ . \tag{36}$$

The integral vanishes because, according to (27), the value of $\epsilon_B(p)$ on the boundary of the region of integration is the constant Fermi energy, μ_B. From this result we learn from (22) and (23) that the space-like components of the ω_μ and $\rho_{\mu 3}$ fields vanish identically,

$$\underset{\sim}{\omega} = \underset{\sim}{\rho}_3 = 0 \tag{37}$$

Therefore, the energy eigenvalues (19–20) simplify and depend only on p through $p = |\underset{\sim}{p}|$. This means that the Fermi surface defined by (27) is a sphere characterized by $k_B = |\underset{\sim}{k}_B|$, and

henceforth we can drop the Θ_B factor in expressions like (32) and perform an integration over the Fermi sphere instead. Next, the normalization of the state $\underset{\sim}{p},\mu$ can be derived by taking the derivative of (34) with respect to ω_0. This yields

$$<B^\dagger B>_{\underset{\sim}{p}\mu} = 1 \tag{38}$$

Hence

$$n_B \equiv <B^\dagger B> = \sum_\mu \int_0^{k_B} \frac{d^3p}{(2\pi)^3} <B^\dagger B>_{\underset{\sim}{p}\mu} = (2J_B + 1)\frac{k_B^3}{6\pi^2} \tag{39}$$

expresses the number density of baryon type B in terms of k_B and its spin J_B. This result could have been anticipated but is derived to give explicit meaning to what follows.

To evaluate the scalar density, which is the source of the σ field (21), take a derivative with respect to m_B, obtaining

$$<\bar{B}B>_{\underset{\sim}{p}\mu} = \frac{\partial \epsilon_B(p)}{\partial m_B} = \frac{m_B - g_{\sigma B}\,\sigma}{\sqrt{p^2+(m_B - g_{\sigma B}\,\sigma)^2}}\,, \tag{40}$$

where in view of (37)

$$\epsilon_B(p) = g_{\omega B}\,\omega_0 + g_{\rho B}\,\rho_{03}\,I_{3B} + E_B(p)\,, \tag{41}$$

$$E_B(p) = \sqrt{p^2 + (m_B - g_{\sigma B}\,\sigma)^2}\,.$$

Consequently,

$$<\bar{B}\,B> = \frac{2J_B+1}{2\pi^2}\int_0^{k_B} p^2dp\,\frac{m_B - g_{\sigma B}\,\sigma}{\sqrt{p^2+(m_B - g_{\sigma B}\,\sigma)^2}}\,. \tag{42}$$

With the foregoing results the mean field equations take the explicit forms,

$$m_\sigma^2\sigma = -\frac{dU}{d\sigma} + \sum_B \frac{2J_B+1}{2\pi^2} g_{\sigma B}\int_0^{k_B} p^2dp\,\frac{m_B - g_{\sigma B}\,\sigma}{\sqrt{p^2+(m_B - g_{\sigma B}\,\sigma)^2}} \tag{43}$$

$$m_\omega^2\omega_0 = \sum_B g_{\omega B}\,n_B \tag{44}$$

$$m_\rho^2\,\rho_{03} = \sum_B g_{\rho B}\,I_{3B}\,n_B \tag{45}$$

with n_B given by (39).

VI. Energy Density and Pressure

Once the system of equations developed above has been solved, the energy density and pressure can be calculated from the canonical expression for the stress-energy tensor,

$$\mathcal{T}_{\mu\nu} = -g_{\mu\nu}\mathcal{L} + \sum \frac{\partial \mathcal{L}}{\partial(\partial^\mu \phi)}\,\partial_\nu\phi \tag{46}$$

where the sum is over the various fields. This yields for the hadronic energy density and

pressure

$$\rho = -\bar{\mathscr{L}} + \sum_B \langle \bar{B}\gamma_0 p_0 B\rangle + (\partial_0 \underset{\sim}{\pi})^2 \tag{47}$$

$$p = \bar{\mathscr{L}} + \sum_B \langle \bar{B}\gamma_i p_i B\rangle + (\partial_i \underset{\sim}{\pi})^2 \ , \quad \text{(i unsummed)} \tag{48}$$

where $\bar{\mathscr{L}}$ is the mean value of the strong interaction Lagrangian

$$\bar{\mathscr{L}} = -\frac{1}{2} m_\sigma^2 \sigma^2 - U(\sigma) + \frac{1}{2} m_\omega^2 \omega_0^2 + \frac{1}{2} m_\rho^2 \rho_{03}^2 \tag{49}$$

The contribution of free pions vanishes in $\bar{\mathscr{L}}$. For free charged pions in the zero momentum state we have for the pion field πutilde, $\pi_1 = \bar{\pi}\cos k_0 t$, $\pi_2 = \bar{\pi}\sin k_0 t$, $\pi_3 = 0$. The field equation of course gives $k_0 = m_\pi$. The charge density of pions from (16) is $n_\pi = (\underset{\sim}{\pi} \times \partial_0 \underset{\sim}{\pi})_3$. Hence

$$k_0 = m_\pi, \ \underset{\sim}{k} = 0, \ (\partial_0 \underset{\sim}{\pi})^2 = \bar{\pi}^2 m_\pi^2 \equiv n_\pi m_\pi, \quad (\partial_i \underset{\sim}{\pi})^2 = 0 \tag{50}$$

For the single-particle energies we have

$$\sum_B \langle \bar{B}\gamma_0 p_0 B\rangle = \sum_B (2J_B + 1)\int \frac{d^3p}{(2\pi)^3}\, \epsilon_B(p)$$

$$= m_\omega^2 \omega_0^2 + m_\rho^2 \rho_{03}^2 + \sum_B \frac{2J_B + 1}{2\pi^2} \int_0^{k_B} p^2 dp \sqrt{p^2 + (m_B - g_{\sigma B}\sigma)^2} \tag{51}$$

where (39), (44), and (45) were used in the last step. To calculate the single-particle contribution to the pressure we calculate from (34)

$$\langle \bar{B}\, \chi\, B\rangle_{p\mu} = \frac{\partial \epsilon_B(p)}{\partial \underset{\sim}{p}} = \frac{\underset{\sim}{p}}{\sqrt{p^2 + (m_B - g_{\sigma B}\sigma)^2}} \tag{52}$$

Hence

$$\langle \bar{B}\, \underset{\sim}{\chi} \cdot \underset{\sim}{p}\, B\rangle = \frac{2J_B + 1}{2\pi^2} \int_0^{k_B} \frac{p^4}{\sqrt{p^2 + (m_B - g_{\sigma B}\sigma)^2}}\, dp \tag{53}$$

Therefore, the total energy density and pressure including leptons are

$$\rho = U(\sigma) + \frac{1}{2} m_\sigma^2 \sigma^2 + \frac{1}{2} m_\omega^2 \omega_0^2 + \frac{1}{2} m_\rho^2 \rho_{03}^2 + n_\pi m_\pi$$

$$+ \sum_B \frac{2J_B + 1}{2\pi^2} \int_0^{k_B} \sqrt{p^2 + (m_B - g_{\sigma B}\sigma)^2}\, p^2 dp$$

$$+ \sum_\lambda \frac{1}{\pi^2} \int_0^{k_\lambda} \sqrt{p^2 + m_\lambda^2}\, p^2 dp \tag{54}$$

$$p = -U(\sigma) - \frac{1}{2}\ m_\sigma^2\,\sigma^2 + \frac{1}{2}\,m_\omega^2\,\omega_0^2 + \frac{1}{2}\,m_\rho^2\,\rho_{03}^2$$

$$+ \frac{1}{3}\sum_B \frac{2J_B+1}{2\pi^2}\int_0^{k_B} \frac{p^4}{\sqrt{p^2 + (m_B - g_{\sigma B}\,\sigma)^2}}\,dp$$

$$+ \frac{1}{3}\sum_\lambda \frac{1}{\pi^2}\int_0^{k_\lambda} \frac{p^4}{\sqrt{p^2 + m_\lambda^2}}\,dp \qquad (55)$$

The extension of the theory to finite temperature is straightforward.[11]

VII. Parameters of the Theory

As is well known in this kind of theory[1,2], saturation of symmetric nuclear matter is achieved by the σ and ω_0 meson. The former reduces the effective mass of the baryon

$$m_B^* = m_B - g_{\sigma B}\sigma \qquad (56)$$

thus lowering the contributions of the single-particle energies, while the repulsive quadratic term in $\omega_0^2$is, by virtue of (44), proportional to n^2.

At the saturation point of nuclear matter only the neutron and proton states will be populated. They are equally coupled to the meson fields. One can see from (43–45) that the field variables are $g_\sigma\sigma$, $g_\omega\omega$, and $g_\rho\rho_{03}$, and that the solution depends on coupling constants and masses only through the ratios $(g_\sigma/m_\sigma)^2$, $(g_\omega/m_\omega)^2$, and $(g_\rho/m_\rho)^2$.

For symmetric matter the leptons are omitted and proton and neutron densities are equal. The four bulk properties of nuclear matter together with the choice of an effective mass at saturation can be used to determine the five parameters of the Lagrangian. With the parameters[7]

$$(g_\sigma/m_\sigma)^2 = 9.957\ \text{fm}^2,\ \ (g_\omega/m_\omega)^2 = 5.354\ \text{fm}^2 \qquad (57)$$

$$(g_\rho/m_\rho)^2 = 6.2\ \text{fm}^2,\ \ b = 0.00414,\ \ c = 0.00716$$

we obtain the correct saturation density 0.145 fm^3, binding energy 15.95 MeV, a compression modulus K = 285 MeV, and charge symmetry coefficient of 36.8 MeV in accord with the droplet model of atomic masses.[20] The effective mass is $m^*/m = 0.77$, which is in the expected range.[4] The binding energy as a function of density corresponding to the above parameters is shown in Fig. 1.

The coupling strength of the isobars and the hyperons to the meson fields are of course not determined by the properties of normal matter. We characterize these parameters as the ratio of coupling constant for the Δ or hyperons to the nucleon coupling constant,

$$x_\Delta = g_{\Delta\sigma}/g_{N\sigma},\ \ x_H = g_{H\sigma}/g_{N\sigma} \qquad (58)$$

and similarly for the coupling to the ω and ρ mesons. For the hyperons we adopt the value of x_H obtained by Moszkowski[16] on the basis of the strange and non-strange quark content of the baryons. This yields $x_H^2 = 2/3$. We will test the dependence of the theory on this parameter by also investigating the case of universal coupling, $x_H = 1$. We adopt the same coupling for the Δ as for the nucleons, i.e., $x_\Delta = 1$.

VIII. Charge Neutrality and Isospin Symmetry

The raison d'etre of a neutron star is the constraint of charge neutrality. For stars in the main sequence and through the evolution to the white dwarf stage, the symmetry energy of nuclei is compatible with charge neutrality. However, an idealized neutron star is highly isospin asymmetric. The asymmetry is resisted by the interaction of baryons with the neutral ρ meson. Its amplitude is driven by the 3-component of the total isospin density according to (45). This provides a quadratic restoring term in the energy density (51),

$$\frac{1}{2} m_\rho^2 \rho_{03}^2$$

which in ordinary nuclei is proportional to $(N - Z)^2$ and contributes, along with the difference in Fermi energies of neutrons and protons, to the symmetry energy in nuclei. The coupling in our model is chosen, as mentioned already, to yield the correct symmetry energy coefficient.

Because of the opposition of charge neutrality and the isospin symmetry energy of neutral matter, it is worth recalling that charge neutrality is an absolute constraint, since it is imposed by long-range forces. If the net charge on a star is Ze and an additional charged particle of mass m and charge e of the same sign is added, stability requires that

$$\frac{G(Am)m}{R} \geqslant \frac{Ze^2}{R} \tag{59}$$

where the star's mass is represented by Am. For net positive (proton) or negative (electron) charge, this means

$$Z/A \lesssim \begin{cases} 10^{-36} & \text{(positive)} \\ 10^{-39} & \text{(negative)} \end{cases} \tag{60}$$

Effectively the charge density must be zero and the short-range interactions must operate within this constraint. Accordingly, baryon populations will arrange themselves in such a way as to minimize the energy density and in accord with charge neutrality. In particular, the isospin symmetry energy will disfavor baryons of the same sign of isospin projection as the neutron. This can be inferred from (41) and (45). Conversely it will favor those with the opposite isospin projection. Other factors affecting the populations of the various baryon species are the baryon masses, electric charges, and other interactions. The precise manner in which these factors determine the particle thresholds is explicit in (27) and (41) which relation will be employed later in understanding the outcome of the numerical solutions.

IX. Electron Chemical Potential

As discussed in section III, the condensation of negative pions in charge-neutral matter imposes an upper bound on the electron chemical potential. This bound will of course depend on the pion-baryon interactions (cf. eq. (14)). In this work we are going to neglect these interactions. We therefore need to discuss the behavior of μ_e in various systems in order to gauge the effect of our approximation on the hyperon populations. This turns out to be straightforward.

First, however, we discuss why our present problem becomes extremely complicated by the π-B interactions. If pion condensation occurs in an interacting system it is because of the attractive p-wave interaction in the π-N system, the interaction being repulsive in the s-state.[18] As has been discussed in detail elsewhere, the p-wave interaction distorts the Fermi seas of the baryons.[7-9] As a consequence their densities cannot be characterized simply by Fermi momenta. The distortion of the Fermi seas of all baryons has to be solved self-consistently with the field equations for the mesons. This problem has been solved for simpler systems, for symmetric nuclear matter[7] and for stable charge-neutral neutron star matter in which, of the baryons, *only* the proton and neutron were considered.[8,9] The behavior of the electron chemical potential in the latter case is shown in Fig. 2. It saturates and at an energy larger than for free pions, which

occurs instead at m_π. The reason for this is that the attractive part of the interaction is p-wave, requiring therefore a finite kinetic energy ($k \neq 0$). The behavior of μ_e in the presence of a condensate of free π^- mesons is also shown in Fig. 2. For this calculation all baryon types of Table I were introduced.

We can study another case, that in which pions do not condense. This situation would occur if the π-N interaction were strongly repulsive. Then (14) could not be satisfied at any density. We can realize this situation by arbitrarily increasing the value of m_π. The behavior of μ_e in the case of no pion condensation, in our system including all baryons of Table I, is also shown in Fig. 2. The electron chemical potential still saturates but at a larger value, around 195 MeV. The reason for saturation in this case is that for sufficiently large baryon densities (>0.5 fm^3) charge neutrality is achieved most economically *among* the baryon populations with only a very small negatively charged lepton population. That is*

$$n + n \rightarrow n + \Lambda$$

becomes more economical than

$$n \rightarrow p + e^- \text{ or } n \rightarrow p + \mu^- .$$

From these considerations we may infer that if μ_e does not reach an upper bound because of pion condensation it will do so because of the growth of heavier baryon populations. We find this upper bound to be $\sim$200 MeV, far less than all meson masses save that of the pion. Therefore the discussion of section III can be extended. The possibility of phase transitions corresponding to mesons that are not driven by finite baryon currents in the *normal* state are foreclosed by the existence of heavier baryons. The π^- phase transition is also foreclosed for the same reason unless (14) has a solution for k that is real when $k_0 = \mu_e \lesssim 200$ MeV. Therefore the two cases corresponding to the lower and upper curves of Fig. 2 may be considered bounds on the possible behavior of μ_e. These two bounds correspond to the condensation of free pions and to no pion condensation, respectively. We shall examine the hyperon populations in the two limiting cases and are able to claim that whatever the π-B interaction the case of condensation of free pions yields the *lower* bound on the hyperon admixture.

*As can be inferred from our discussion of chemical equilibrium, the associated kaon produced in such a reaction does not need to be mentioned.

X. Properties of Dense Neutron Star Matter

In this section the properties and composition of stable charge-neutral (neutron star) matter are presented together with comparisons that bring out the roles of the isospin symmetry property of the interactions, of the hyperons and of the π^- condensate.

For the above purpose the following cases will be studied, the first of which is the complete theory as described in sections IV - VI and with parameters as in section VII. We characterize the cases by the particle content and any modifications to the standard coupling constants discussed in Section VII. They are,

1) n, p, hyperons, Δ, e, μ^-, π^-.

2) n, p, hyperons, Δ, e, μ^-.

3) like 2) but universal coupling of hyperons ($x_H = 1$).

4) like 3) but $g_\rho = 0$.

5) n, p, e, μ^-.

6) like 5) but $g_\rho = 0$.

7) n, p, e, μ^-, π^-.

8) n, $g_\rho = 0$.

9) Symmetric nuclear matter.

Comparison between case 1 and case 2 will illustrate the effect of a π^- condensate, while case 3 tests the dependence on the coupling of the hyperons, as discussed in section VII. We are not aware of any previous calculations of neutron star structure that employ nuclear forces that are known to yield the empirical symmetry energy of ordinary nuclei as the present theory does. Case 4 will illustrate the effect of underestimating the isospin symmetry energy when compared with case 3. Case 5 corresponds to a theory for which the ρ-meson coupling yields the correct symmetry energy in nuclear matter but in which the possible presence of pions, isobars and hyperons is ignored. This case in comparison with case 1 and 2 illustrates the effects of these particles.

The usual scenario for neutron stars envisages that they contain neutrons in β^- equilibrium with a small number of protons, electrons and μ^-. Cases 5 and 6 are versions of this scenario, the former for which the symmetry energy posseses the correct value in nuclear matter, and the latter for which $g_\rho = 0$ and the symmetry energy is too small. Case 7 is like 5 but free pions are allowed to condense.

Finally case 8 is pure neutron matter with $g_\rho = 0$ and case 9 is symmetric nuclear matter. The binding energy for both these cases are shown in Fig. 1.

We discuss in detail some of these cases below.

Case 1. (The present theory)

The simultaneous non-linear equations (21–30) must be solved for the (8 + N) unknown meson field strengths, chemical potentials and Fermi momenta. However, the complete solution can be presented, once it is found, by showing the dependence on baryon number density n only of the field strengths and the two chemical potentials. The Fermi momenta for the

leptons can be calculated from (28–29) and for the hadrons from (27) using the above quantities. Fig. 3 shows the solution for case 1, which corresponds to our complete theory. We now discuss the solution. The vector field, $g_\omega \omega_0$ is roughly proportional to the baryon density, n, and exactly proportional in the case of universal coupling (cf. Eq. (44)). The saturation of μ_e occurs, as discussed in section III because of the condensation of free π^-. The ρ-field and electron chemical potential behave in roughly the same way as a function of density. At low density, below the μ^-, π^- and hyperon thresholds, charge neutrality can be achieved only among protons and an equal number of electrons. The latter being relativistic, the charge neutrality of a star forces a high isospin asymmetry. In fact from the approximate relations $\mu_n \approx k_n^2/2m$, $\mu_p \approx k_p^2/2m$, $\mu_e \approx k_e$ and the conditions for charge neutrality ($k_p = k_e$) and chemical equilibrium ($\mu_n = \mu_p + \mu_e$) we find, where n_n is the neutron density and m the nuclear mass,

$$\mu_e \approx .06m\,(n_n/n_0)^{\frac{2}{3}}\left[1 - 0.03(n_n/n_0)^{\frac{2}{3}}\right] \tag{61}$$

$$I_3 \approx -\frac{1}{2}n_n\left[1 - 0.005(n_n/n_0)\right] \quad .$$

The ρ-field is driven by the isospin density so both μ_e and ρ_{03} grow as n_n grows *at* low density. However as the thresholds for pions and hyperons are reached, more energetically favorable options for charge neutrality become available. In this regime the role of the ρ-field is to select those options with low isospin density. Consequently, μ_e and ρ_{03} grow less rapidly or saturate as density increases.

The binding energy per nucleon is compared in Fig. 1 with symmetric nuclear matter, with pure neutron matter and with case 5. The latter comparison illustrates the softening effect of the hyperons. We see also that while pure neutron matter, in the absence of coupling to the ρ-meson, is slightly bound, our theory for neutron star matter (stable charge-neutral matter) is not. This is due to the isospin symmetry energy arising from the coupling of the isospin density to the neutral ρ-meson.

The equation of state p vs ρ is shown in Fig. 4 (see also Table IV) and compared with the causality limit $p = \rho$, with an ultrarelativistic gas $p = \rho/3$ and with an ideal neutron gas, which for high density approaches $p = \rho/3$. The units adopted for this figure are related to the nuclear units by

$$197.32\ \text{MeV/fm}^3 = \text{fm}^{-4} = 3.518\ 10^{14}\ \text{g/cm}^3 = 3.162\ 10^{35}\ \text{dyne/cm}^2 \quad .$$

For normal nuclear matter the energy density is

$$\rho_0 \sim 2.48\ 10^{14}\ \text{g/cm}^3 \quad .$$

Below nuclear density our equation of state is softer than an ideal neutron gas because of the attractive interaction but it stiffens around nuclear density because of the increasing importance of the short-range repulsion. The structure in the equation of state in the form of slight softenings at $\log \rho \sim 14.6$ and 15 correspond to the onset of pion condensation and to hyperons. Neither produces an effect as dramatic as has occasionally been speculated upon.[14, 21] The dotted curve corresponds to the situation when π^- and hyperons are rejected (case 5). Asymptotically, our equation of state approaches $p \to \rho$ because the repulsion arises from the exchange of a vector meson. Such a behavior of vector meson interactions has been remarked upon by Zel'dovich.[22] It can be seen explicitly by examining equations (54) for p and ρ in the limit of large density. As $k_B \to \infty$, the mass terms in the integrals can be ignored. The σ-field is bounded by the order of the baryon masses. Then it follows that

$$\rho \rightarrow \frac{1}{2}\left(\sum_B \frac{g_{\omega B}}{m_\omega} n_B\right)^2 + \frac{1}{2}\left(\sum_B \frac{g_{\rho B}}{m_\rho} I_{3B} n_B\right)^2 + \sum_B \frac{2J_B+1}{2\pi^2}\frac{k_B^4}{4} \tag{62}$$

$$p \rightarrow \frac{1}{2}\left(\sum_B \frac{g_{\omega B}}{m_\omega} n_B\right)^2 + \frac{1}{2}\left(\sum_B \frac{g_{\rho B}}{m_\rho} I_{3B} n_B\right)^2 + \frac{1}{3}\sum_B \frac{2J_B+1}{2\pi^2}\frac{k_B^4}{4} \tag{63}$$

Since $n_B \sim k_B^3$ we find that p approaches ρ from below. (The speed of sound, $(dp/d\rho)^{1/2}$, approaches, but is less than that of light.)

It is well known that as a star becomes more dense, the process of neutronization occurs. The range of densities describable by our Lagrangian and our assumption of uniform matter is from the density of a neutron gas, and upward. We study the solutions from $n = 0.04$ fm^{-3} to 1.2 fm^{-3} (i.e., $0.28 \lesssim n/n_0 \lesssim 8$ where $n_0 = 0.145$ fm^{-3} is the normal nuclear density). The evolution of particle populations with increasing baryon density, n, are shown in Fig. 5. At low density (on the nuclear scale) charge neutral matter is almost pure in neutron. As the density rises, high momentum neutrons β-decay into protons and electrons or muons. The μ^- threshold occurs at $n \approx 0.12$ fm^{-3}, just below normal nuclear density, and the π^- threshold occurs at $n \approx 0.18$ fm^{-3}, just above nuclear density. The π^- as already discussed, arrests the growth of the lepton fraction. The π^- fraction grows very rapidly with increasing baryon density to $n \sim 0.4$ fm^{-3}, and then it decreases slowly until $n \sim 1$ fm^{-3} and then it falls precipitously. This occurs as the thresholds for hyperons are reached. These thresholds depend not only on the mass but on the charge and on the interactions with the meson fields σ, ω_0 and ρ_{03}, as seen through equations (25, 27, 41) which we combine to form the threshold equation,

$$\mu_n - q_B \mu_e \geqslant g_{\omega B}\,\omega_0 + g_{\rho B}\,\rho_{03}\,I_{3B} + m_B - g_{\sigma B}\,\sigma \tag{64}$$

When the left side equals or exceeds the right, the baryon species, B, will be populated. From (23) we infer that the sign of $g_{\rho B}\,\rho_{03}$ is fixed by the net isospin density of the star, which is of course that of the neutron. Therefore baryons having the same sign of isospin projection as the neutron are *isospin-unfavored.* Those having the same sign of charge as the proton are *charge-unfavored* because they must appear with another particle of opposite charge to maintain charge neutrality. Those with the same charge as the electron however are *charge-favored* because such a baryon can replace a neutral baryon and an election at the top of the Fermi sea. As a case in point, the Σ^- is charge favored but isospin unfavored, while the Λ, having zero charge and isospin is neutral with respect to both of these effects. The precise way in which these factors balance out depends on the solution of (20–30) which was shown for this case in Fig. 3. The Λ is found to have a somewhat lower threshold than the Σ^-. Nowhere in the density range shown are the Δ's populated. The most favored charge state is the Δ^-, but it is unfavored by its isospin. These two factors contribute an attractive energy in the threshold condition (64) amounting to $-\mu_e - (\frac{3}{2})g_\rho\rho_{03} \geqslant -20$ MeV over the density range $0.2 < n\ \text{fm}^3 < 1.2$. However this is insufficient to overcome its large mass. The $\Delta^{++}$is isospin favored but doubly unfavored by its charge. Together these contribute a repulsive energy $2\mu_e + (\frac{3}{2})g_\rho\rho_{03} \geqslant +70$ MeV over the same density range, which assures its absence. Equation (64) together with the chemical potentials and field strengths shown in Fig. 3 can be used to check that no other baryons than those shown in Fig. 5 can be populated in the density range of that figure. In applying (64) with the field strengths shown in Fig. 3 as $g_\sigma\sigma$, $g_\omega\omega_0$, $g_\rho\rho_{03}$ recall that the hyperon coupling is modified by the factor x_H of Eq. (58).

Case 2. (No pion condensation)

In this case pions do not condense because of an assumed repulsion in their interaction. The behavior of the field strengths and chemical potentials in the absence of pion condensation is shown in Fig. 6. As discussed in Section III the electron chemical potential will saturate

either by reason of increasing charged hyperon populations or because of pion condensation, whichever effect sets in first. Here it occurs through the growth of the hyperon populations. Fig. 7 shows the particle populations. Comparison with Fig. 5 shows that π^- condensation shifts the threshold for the hyperons to somewhat higher density. This is easily understood. If the electron pressure cannot be relieved by π^- condensation, then neutron and electron pressures will be relieved by Σ^-, for example. Fig. 5 and 7 illustrate the point emphasized earlier, that admitting the condensation of free pions will yield a conservative estimate of hyperon populations. The equation of state is presented in Table V.

Case 3 (Universal coupling)

In the preceding two cases, the hyperon couplings were reduced in comparison with the nucleon and isobar couplings as discussed in section VII. This case by comparison shows the results for universal coupling. Fig. 8 shows the field strengths and chemical potentials while Fig. 9 shows the populations. In comparison with Fig. 7 to which this case is otherwise similar, we see that the populations are not excessively effected by the variation of x_H between 1 and 2/3. The equation of state is presented in Table VI. In Table VII the equation of state for a case like 1 but with universal coupling is given for completeness.

Case 4 (Symmetry energy)

Next we demonstrate the extreme importance of the isospin symmetry energy of the system as regards the hyperon populations. Of course such a symmetry energy always exists for Fermions through their kinetic energies. However, this accounts for only a part of the observed symmetry energy coefficient of normal nuclei. The coupling of nucleons to the neutral ρ field (23) provides the rest. By setting the coupling constant of the ρ field to zero we can see the important role played by the isospin symmetry energy. The field strength σ, and the chemical potentials are shown in Fig. 10. In this case μ_e is saturated at about 120 MeV by the hyperons so that pions are unable to condense. The populations are shown in Fig. 11 and contrast sharply with Fig. 5. In particular the Σ^- now has the lowest threshold of the hypersons. It is charge favored as discussed above, and with vanishing ρ-coupling its isospin is not a liability. This case, for which the nucleons, isobars and hyperons are universally coupled, corresponds rather closely to the results of Pandharipande[14] and of Bethe and Johnson.[15] (Compare for example, Fig 8 of Pandharipande). The Δ^- has a low threshold because of the low symmetry energy (g_ρ=0). Since universal coupling of all baryons is assumed for this case, some terms in (64) are common to Δ^- and Λ. Their thresholds are otherwise determined by $(-\mu_e + m_\Delta)$ and m_Λ respectively which are equal at $n \sim 0.508$ fm^{-3}. This is the only case for which we find the presence of an isobar and this occurs because of the artificially low symmetry energy.

Case 5 (no hyperons, Δ or π^- condensate)

Fig. 12 shows how the electron chemical potential is an monotonic increasing function of density in the absence of hyperons or a pion condensate. The particle populations are shown in Fig. 13. Note that in this, as with the preceding cases, the proton density reaches 10–30% in contrast with the usual scenario below, in which the correct charge symmetry is not enforced.

Case 6 (Usual scenario)

Frequently neutron stars are thought of as being composed of neutrons in β equilibrium with a *very small* proton population. This would be the case if the symmetry energy is not large enough compared to its empirical value, and hyperons did not exist. The chemical potentials are shown in Fig. 14, and the particle populations are shown in Fig. 15. The proton population never exceeds 10% in the relevant density range. Compare this with case 5 (Fig. 13) where the symmetry energy for normal matter is correct.

XI. Physical Characteristics of Neutron Star

The physical characteristics of a neutron star, such as mass, radius, energy density profile and critical mass, can be found by solving the Oppenheimer-Volkoff equations, which are the form that Einstein's equations for the gravitational field assume for static spherically symmetric geometries.[23] For a given equation of state, these equations determine the way in which matter will arrange itself. For neutron stars the density of matter spans an enormous range, from super-nuclear densities of $\sim 5 \times 10^{15}$ g/cm^3 in the core down to zero at the edge. However the atmosphere is so thin, indeed so is the crust of all but the least massive stars, that these regions contribute negligibly to the mass, radius and moment of inertia. Most of the mass of the star is contributed by highly compressed matter at nuclear and super-nuclear densities. In Table III we show three density ranges and the source of the equation of state in each. The interior exists in the form of a dense gas of hadrons and leptons and is calculated in this work. The inner surface is believed to consist of a lattice of extremely neutron rich heavy metals immersed in a neutron and a relativistic electron gas. The equation of state in this region is taken from the work of Negele and Vautherin.[24] The outer surface consists of a lattice of lighter metals immersed in an electron gas, and the equation of state in this region is taken from Harrison and Wheeler.[25] The equation of state over all three regions is shown in Fig. 16. The detail of the baryon gas region in which the bulk of all but the least massive stars lies, was shown in Fig. 4, and is tabulated in Table IV.

For a given equation of state of matter, the Oppenheimer-Volkoff equations have a unique solution that depends on a single parameter characterizing the conditions of matter at the center. This can be chosen as the baryon density, or energy density for example. The mass of neutrons stars in our theory (case 1) as a function of the central density of the star is shown in Fig. 17 together with the moment of inertia. The effect on the mass and moment of inertia of the suppressing the π^- condensate and hyperons are each shown for comparison. The hyperons have the larger effect. The mass is an increasing function of central density up to a critical maximum value, known as the Oppenheimer-Volkoff limit. Beyond this mass the star is unstable to gravitational collapse. The maximum mass in our theory is M $\sim$ 1.81 solar masses which occurs for a central density of 2.4×10^{15} g/cm^3, or a baryon number density of 1.088 fm^{-3}, about eight times nuclear density. The radius of this star is about 11.3 km. With the suppression of the pion condensate and hyperons, this limit increases to M $\sim$ 2.15 solar masses corresponding to a central density of 2.13×10^{15} g/cm^3 or baryon density of 0.943 fm^{-3}. Stars with larger central density than the one with maximum mass are unstable to gravitational collapse. Both the maximum mass and moment of inertia in our theory exceed the observational lower bounds.[26] Some of the characteristics of stars in our theory for various central densities can be found in Tables VIII – XI.

The minimum mass of a neutron star in our theory is 0.094 solar masses, and has a central density of 1.09 10^{14} g/cm^3 or 0.065 baryons per fm^3. All neutron stars therefore have central densities lying in the hadron gas region, and for all but the least massive, 95% or more of the mass of the star is composed of matter that lies at densities in this range (region III of Table III), as we shall show below. For central densities less than the above minimum value down to the white dwarf region of $\rho < 10^9$ g/cm^3 there are no stable stellar objects. The first entry in Table VIII lies at the upper end of this unstable region and by contrast with the next entry shows the sudden transition to stability.

The dependence of radius on mass (and therefore central density) shown in Fig. 18 reflects the vanishing of stability at the lower limit of the neutron star region by the rapid growth in size as the lower limit is approached from above. Over the greatest range however, the neutron star is composed of highly compacted matter with a radius of 13 $\pm$ 2 km. The compactness is illustrated also in Fig. 19 which shows the density profile as a function of radius for four neutron stars ranging from our most massive one to the least massive one. Only for stars with central densities near the lower limit does the star possess a thick crust. The dot on each curve shows the radius interior to which 95% of the star's mass is contained. The three density

regimes marked on this figure correspond to those of Table III. The break in the slope of density profile visible in Fig. 19 for the lighter stars, that occurs at 4×10^{11} g/cm^3 corresponds to the end point of the neutron drip region. This point is clearly visible in the equation of state shown in Fig. 16. The atomic number over the range of stable neutron star masses can be seen in Fig. 18.

In the presence of the strong gravitational field of a neutron star the metric is altered from the locally flat metric $g_{\rho\sigma} = \delta_{\rho\sigma}\,(1, -1, -1, -1)$, in which the equation of state of matter was solved. In spherically symmetric geometry it has the Schwartzchild form

$$g_{\sigma\rho} = \delta_{\sigma\rho}\,(e^{\nu(r)}, -e^{\lambda(r)}, -r^2, -r^2 \sin^2\theta) \tag{65}$$

The radial metric function is given by

$$e^{-\lambda(r)} = 1 - (8\pi/r)\int_0^r \rho(r)\, r^2 dr \tag{66}$$

At the surface of the star $e^{\nu(R)} = e^{-\lambda(R)}$. The fractional red shift in the wavelength of light emitted from the surface is $z = e^{\nu(R)/2} - 1$ and reaches a value of about 40 percent for the star of case 1 (see Fig. 20 and Table VIII). This red shift is fairly close to the upper limit of 61.5 percent obtained by Bondi[27] for *stable* compact objects. If the hyperons and pion condensate are artificially suppressed (case 5) then the fractional redshift, shown by the dotted line in Fig. 24 almost reaches Bondi's limit.

XII. Hyperon Populations

The populations of various hadrons as a function of position in the star can be inferred by noting the unique connection between population and baryon density or equivalently energy density and in turn the connection for a particular star that exists between energy density and position in the star that is provided by the solution to the Oppenheimer-Volkoff equations. This connection provides the proper number density, $n_B(r)$ for particle species B as would be measured in a locally inertial reference frame at a distance r from the center. The total number of species B in a particular star is given by

$$N_B = 4\pi \int_0^R n_B\,(r)\, e^{\lambda(r)/2}\, r^2 dr \tag{67}$$

where R is the radius and $e^{\lambda(r)/2}$ is the radial metric function for the star in question. For two stars of our theory, the one at the upper limit in mass, 1.81 $M_\odot$ and one of mass 1.53 $M_\odot$, we show in an "onion skin" depiction, the *proper* number densities of the various particles as a function of position in the star in Figs. 20 and 21. Of particular note is the paucity of leptons. Charge neutrality is achieved in this theory by a balance of charges on relatively large populations of charged hadrons. The star's interior is dominated by hyperons. However, the total hyperon fraction, depicted in Fig. 22, as a function of star mass reaches a maximum value of 15% for the most massive neutron star. Here we see that the hyperon fraction, which is zero for stars whose central density is below a critical value ($n \sim 0.4$ fm^{-3}, cf Fig. 5), grows extremely rapidly above the threshold. The terminal point corresponds to the most massive neutron star in stable hydrostatic equilibrium. The situation is only slightly altered if pions do not condense (for example by virtue of a large repulsive self-energy in the medium). This is our case 2 for which Fig. 23 shows the populations in a heavy neutron star. In this case the hyperon fraction reaches a maximum value of 22% (see Fig. 22) and confirms our assertion in section IX that allowing free pions to condense will provide a conservative estimate of the hyperon content of neutron stars.

It is interesting to contrast all of the cases where hyperons are present to a case where they are eliminated from the calculation. Then if pions do not condense, a large population of leptons appears in the star, Fig. 24, while in the case that pions are free to condense, they do so with a very large population, and quench the lepton populations, Fig. 25.

Discussion and Conclusion

We have described a theory of dense stable charge-neutral matter that has a number of attractive properties. Based on this theory we investigated the structure of neutron stars, and elucidated the role of various features.

The description employs a Lagrangian field theory of interacting nucleons, hyperons and the relevant mesons, which is solved in the mean field approximation. The completeness of the theory with respect to the number of meson fields was discussed. The σ, ω and ρ^0 mesons are coupled to nucleon currents which have a non-zero expectation value in the normal ground state of isospin asymmetric matter and consequently these mesons have finite amplitudes in the medium. Mesons with other quantum numbers, such as the π, $\rho^{\pm}$, K, K*, are coupled to currents which have vanishing expectation value in the normal ground state, by virtue of the quantum numbers that they carry. Therefore, they are absent in the ground state of the star because they can decay freely, unless a phase transition occurs which endows the current to which they are coupled with a finite value. We pointed out that phase transitions involving mesons more massive than the pion are precluded by either π^- condensation or by the growth of hyperon populations, whichever sets in first. Consequently, such mesons can play no role in the ground state of a neutron star.

Neutron stars have usually been studied in the non-relativistic Schroedinger theory. Such a theory can yield an equation of state for matter at high density in which the sound velocity exceeds that of light. Since relativistic covariance of the present theory was retained throughout, our equation of state automatically respects causality.

The present theory correctly describes the bulk properties of normal nuclear matter. Of special importance for neutron stars, it yields the empirical value of the symmetry energy coefficient in nuclear matter. In principle the non-relativistic Schroedinger theory, employing nuclear forces that agree with observed two-nucleon scattering parameters, may also yield the correct symmetry energy coefficient. In practice the theory has not yet converged on the correct saturation density and binding energy, and the symmetry energy is therefore uncontrolled, and frequently not calculated. Aside from the contribution of kinetic energies to the symmetry energy it is the coupling of the neutral ρ-meson to the $3-$ component of the isospin density that favors isospin symmetry in our theory. Therefore in addition to the obvious role of the symmetry energy in raising the energy of neutron star matter compared to symmetric matter, the ρ-meson plays a very important part in determining the particle populations by favoring an admixture with small isospin density.

We find that in the cores of the heaviest neutron stars, hyperons are more numerous than nucleons and that in the star as a whole, 15-20% of all baryons are hyperons. The lower figure corresponds to the case where a pion condensate is allowed to develop and the higher figure to the case where it does not. The presence or absence of a pion condensate therefore is not crucial to our conclusion concerning the presence of a significant hyperon population.

It is interesting that, independent of pion condensation, the lepton population is strongly suppressed by hyperons. This may have a strong effect on the electrical conductivity; it will be lower if hyperons are present than if they are absent. The electrical conductivity in turn determines the decay rate of the strong magnetic field needed to produce the pulsar beam effect. Consequently the presence of hyperons in a pulsar may register itself in the active lifetime of the pulsar. This is estimated from astrophysical data to be less than several million years.[26] In a subsequent work, the conductivity and decay constant of the magnetic field in pulsars will be calculated.

It has long been known that the maximum neutron star mass (Oppenheimer-Volkoff limit) of a theory is of interest for two reasons. The first is that some neutron star masses are known and the largest of these imposes a lower bound on the maximum mass of theoretical models. The current lower bound is about 1.5 ± 0.1 solar masses. The other reason is that the maximum mass can be useful in identifying black hole candidates.[28] Thus if the mass of a compact companion of an optical star is determined to exceed the maximum mass of a neutron star it must be a black hole. The maximum mass of stable neutron stars in our theory lies in a narrow range of 1.79 to 1.98 solar masses (see Fig. 22) with 1.81 corresponding to case 1 which we consider to be our best estimate. The variation about this figure corresponds to the presence or absence of a pion condensate and the assumption of universal baryon coupling or to a reduced coupling for hyperons as motivated by quark counting arguments. For comparison if hyperons, isobars and pion condensate are suppressed, the limiting mass increases to 2.15 solar masses. On the other hand Pandharipande's[14] equation of state for hyperon matter is much softer than ours and leads to a limiting mass of 1.41 solar masses.[29] Most theoretical models yield limiting masses in the range 1.3 to 1.8.[29] All of these are considerably lower than a variational upper bound[30] of 3.2 and therefore appear to provide a useful consensus on the limiting mass, as being somewhat less than two solar masses.

Table I.
The six lowest-mass baryon multiplets, their quantum numbers and charges

	m	Y	J	I	I_3	q
N	938	1	$\frac{1}{2}$	$\frac{1}{2}$	$\frac{1}{2}$	1
					$-\frac{1}{2}$	0
Λ	1116	0	$\frac{1}{2}$	0	0	0
Σ	1193	0	$\frac{1}{2}$	1	1	1
					0	0
					-1	-1
Δ	1232	1	$\frac{3}{2}$	$\frac{3}{2}$	$\frac{3}{2}$	2
					$\frac{1}{2}$	1
					$-\frac{1}{2}$	0
					$-\frac{3}{2}$	-1
Ξ	1318	-1	$\frac{1}{2}$	$\frac{1}{2}$	$\frac{1}{2}$	0
					$-\frac{1}{2}$	-1
Ω	1672	-2	$\frac{3}{2}$	0	0	-1

Table II.

Partial list of mesons ordered as to quantum numbers and the corresponding part of the interaction Lagrangian. The parenthenses enclose the various baryon currents to which the mesons are coupled.

Meson	J^π	I	$\|S\|$	$\mathscr{L}^{int}$
σ	0^+	0	0	$g_\sigma \sigma(\bar{B}B)$
ω	1^-	0	0	$g_\omega \omega_\mu(\bar{B}\,\gamma^\mu\,B)$
π	0^-	1	0	$g_\pi \underset{\sim}{\pi}(\bar{B}\gamma_5\,\underset{\sim}{\tau}\,B)$
ρ	1^-	1	0	$g_\rho\,\underset{\sim}{\rho}_\mu\,(\bar{B}\gamma^\mu\,\underset{\sim}{\tau}\,B)$
K	0^-	1/2	1	$g_K K(\bar{\Lambda}\,\gamma_5\,N)\ldots$
K*	1^-	1/2	1	$g_K\,K^*_\mu\,(\underset{\sim}{\bar{\Sigma}}\cdot\underset{\sim}{\tau}\,\gamma^\mu\,N)\ldots$

Table III.
Three density regions (g/cm^3) needed to describe the neutron star surface I and II and the star interior, III.

I	$2 \times 10^3 < \rho < 1 \times 10^{11}$	Harrison and Wheeler (ref. 25)
II	$1 \times 10^{11} < \rho < 2 \times 10^{13}$	Negele and Vautherin (ref. 24)
III	$2 \times 10^{13} < \rho < 5 \times 10^{15}$	This work

Table IV
Equation of state for case 1.

n (fm^{-3})	ρ (g/cm^3)	p ($dynes/cm^2$)	n (fm^{-3})	ρ (g/cm^3)	p ($dynes/cm^2$)
.04	6.7232 +13	1.6213 +32	.84	1.7197 +15	3.4950 +35
.06	1.0101 +14	4.8916 +32	.86	1.7702 +15	3.6644 +35
.08	1.3495 +14	1.1390 +33	.88	1.8211 +15	3.8384 +35
.10	1.6914 +14	2.2044 +33	.90	1.8724 +15	4.0135 +35
.12	2.0361 +14	3.7258 +33	.92	1.9241 +15	4.1855 +35
.14	2.3840 +14	5.6872 +33	.94	1.9763 +15	4.3594 +35
.16	2.7354 +14	8.1769 +33	.96	2.0289 +15	4.5353 +35
.18	3.0903 +14	1.0528 +34	.98	2.0819 +15	4.7120 +35
.20	3.4482 +14	1.2910 +34	1.00	2.1353 +15	4.8907 +35
.22	3.8086 +14	1.5867 +34	1.02	2.1891 +15	5.0725 +35
.24	4.1727 +14	1.9456 +34	1.04	2.2433 +15	5.2575 +35
.26	4.5403 +14	2.3708 +34	1.06	2.2979 +15	5.4459 +35
.28	4.9122 +14	2.8650 +34	1.08	2.3529 +15	5.6382 +35
.30	5.2879 +14	3.4314 +34	1.10	2.4083 +15	5.8339 +35
.32	5.6682 +14	4.0714 +34	1.12	2.4641 +15	6.0334 +35
.34	6.0531 +14	4.7866 +34	1.14	2.5203 +15	6.2374 +35
.36	6.4429 +14	5.5793 +34	1.16	2.5769 +15	6.4442 +35
.38	6.8379 +14	6.4505 +34	1.18	2.6339 +15	6.6525 +35
.40	7.2383 +14	7.3893 +34	1.20	2.6913 +15	6.8638 +35
.42	7.6439 +14	8.2933 +34	1.22	2.7491 +15	7.0781 +35
.44	8.0541 +14	9.1960 +34	1.24	2.8108 +15	7.2957 +35
.46	8.4689 +14	1.0082 +35	1.26	2.8733 +15	7.5177 +35
.48	8.8882 +14	1.0998 +35	1.28	2.9361 +15	7.7431 +35
.50	9.3118 +14	1.1952 +35	1.30	2.9994 +15	7.9730 +35
.52	9.7399 +14	1.2948 +35	1.32	3.0631 +15	8.2067 +35
.54	1.0172 +15	1.3989 +35	1.34	3.1272 +15	8.4448 +35
.56	1.0609 +15	1.5076 +35	1.36	3.1918 +15	8.6870 +35
.58	1.1050 +15	1.6212 +35	1.38	3.2568 +15	8.9333 +35
.60	1.1495 +15	1.7396 +35	1.40	3.3221 +15	9.1840 +35
.62	1.1945 +15	1.8630 +35	1.42	3.3879 +15	9.4395 +35
.64	1.2400 +15	1.9915 +35	1.44	3.4541 +15	9.6991 +35
.66	1.2859 +15	2.1251 +35	1.46	3.5208 +15	9.9635 +35
.68	1.3323 +15	2.2638 +35	1.48	3.5877 +15	1.0232 +36
.70	1.3791 +15	2.4078 +35	1.50	3.6552 +15	1.0505 +36
.72	1.4264 +15	2.5570 +35	1.52	3.7227 +15	1.0783 +36
.74	1.4742 +15	2.7065 +35	1.54	3.7910 +15	1.1066 +36
.76	1.5224 +15	2.8572 +35	1.56	3.8596 +15	1.1353 +36
.78	1.5711 +15	3.0111 +35	1.58	3.9286 +15	1.1645 +36
.80	1.6202 +15	3.1683 +35	1.60	3.9982 +15	1.1941 +36
.82	1.6697 +15	3.3296 +35	1.62	4.0679 +15	1.2242 +36

Table V
Equation of state for case 2.

n (fm^{-3})	ρ (g/cm^3)	p ($dynes/cm^2$)	n (fm^{-3})	ρ (g/cm^3)	p ($dynes/cm^2$)
.04	6.7232 +13	1.6213 +32	.58	1.1113 +15	1.5348 +35
.06	1.0101 +14	4.8916 +32	.60	1.1557 +15	1.6496 +35
.08	1.3495 +14	1.1390 +33	.62	1.2006 +15	1.7699 +35
.10	1.6914 +14	2.2044 +33	.64	1.2459 +15	1.8956 +35
.12	2.0360 +14	3.7261 +33	.66	1.2916 +15	2.0267 +35
.14	2.3840 +14	5.6872 +33	.68	1.3378 +15	2.1632 +35
.16	2.7354 +14	8.1772 +33	.70	1.3845 +15	2.3023 +35
.18	3.0906 +14	1.1248 +34	.72	1.4316 +15	2.4415 +35
.20	3.4501 +14	1.4940 +34	.74	1.4791 +15	2.5837 +35
.22	3.8139 +14	1.9290 +34	.76	1.5271 +15	2.7298 +35
.24	4.1826 +14	2.4327 +34	.78	1.5755 +15	2.8801 +35
.26	4.5562 +14	3.0074 +34	.80	1.6243 +15	3.0348 +35
.28	4.9351 +14	3.6556 +34	.82	1.6736 +15	3.1939 +35
.30	5.3192 +14	4.2700 +34	.84	1.7233 +15	3.3580 +35
.32	5.7076 +14	4.8473 +34	.86	1.7735 +15	3.5269 +35
.34	6.1002 +14	5.4507 +34	.88	1.8241 +15	3.7005 +35
.36	6.4967 +14	6.0394 +34	.90	1.8751 +15	3.8791 +35
.38	6.8967 +14	6.6576 +34	.92	1.9266 +15	4.0549 +35
.40	7.3009 +14	7.3140 +34	.94	1.9785 +15	4.2304 +35
.42	7.7086 +14	8.0131 +34	.96	2.0308 +15	4.4088 +35
.44	8.1199 +14	8.7572 +34	1.00	2.1367 +15	4.7718 +35
.46	8.5354 +14	9.5483 +34	1.04	2.2443 +15	5.1537 +35
.48	8.9547 +14	1.0388 +35	1.08	2.3535 +15	5.5518 +35
.50	9.3779 +14	1.1277 +35	1.12	2.4645 +15	5.9670 +35
.52	9.8054 +14	1.2217 +35	1.16	2.5770 +15	6.3974 +35
.54	1.0237 +15	1.3208 +35	1.20	2.6913 +15	6.8448 +35
.56	1.0673 +15	1.4251 +35	1.24	2.8073 +15	7.3105 +35

Table VI
Equation of state for case 3.

n (fm^{-3})	ρ (g/cm^3)	p ($dynes/cm^2$)	n (fm^{-3})	ρ (g/cm^3)	p ($dynes/cm^2$)
.04	6.7232 +13	1.6219 +32	.84	1.7689 +15	4.3885 +35
.06	1.0101 +14	4.8894 +32	.86	1.8230 +15	4.6317 +35
.08	1.3495 +14	1.1392 +33	.88	1.8776 +15	4.8749 +35
.10	1.6914 +14	2.2042 +33	.90	1.9330 +15	5.1224 +35
.12	2.0361 +14	3.7261 +33	.92	1.9889 +15	5.3760 +35
.14	2.3840 +14	5.6869 +33	.94	2.0454 +15	5.6366 +35
.16	2.7354 +14	8.1763 +33	.96	2.1026 +15	5.9038 +35
.18	3.0906 +14	1.1248 +34	.98	2.1604 +15	6.1779 +35
.20	3.4501 +14	1.4940 +34	1.00	2.2188 +15	6.4596 +35
.22	3.8139 +14	1.9290 +34	1.02	2.2779 +15	6.7487 +35
.24	4.1826 +14	2.4327 +34	1.04	2.3376 +15	7.0449 +35
.26	4.5562 +14	3.0074 +34	1.06	2.3979 +15	7.3485 +35
.28	4.9351 +14	3.6556 +34	1.08	2.4589 +15	7.6599 +35
.30	5.3196 +14	4.3791 +34	1.10	2.5206 +15	7.9790 +35
.32	5.7094 +14	5.1338 +34	1.12	2.5829 +15	8.3053 +35
.34	6.1044 +14	5.8042 +34	1.14	2.6459 +15	8.6392 +35
.36	6.5034 +14	6.5083 +34	1.16	2.7095 +15	8.9810 +35
.38	6.9072 +14	7.2675 +34	1.18	2.7737 +15	9.3301 +35
.40	7.3157 +14	8.0890 +34	1.20	2.8387 +15	9.6874 +35
.42	7.7290 +14	8.9772 +34	1.22	2.9043 +15	1.0052 +36
.44	8.1470 +14	9.9344 +34	1.24	2.9706 +15	1.0424 +36
.46	8.5702 +14	1.0963 +35	1.26	3.0375 +15	1.0804 +36
.48	8.9983 +14	1.2064 +35	1.28	3.1052 +15	1.1192 +36
.50	9.4318 +14	1.3239 +35	1.30	3.1735 +15	1.1587 +36
.52	9.8708 +14	1.4491 +35	1.32	3.2425 +15	1.1990 +36
.54	1.0315 +15	1.5819 +35	1.34	3.3122 +15	1.2401 +36
.56	1.0765 +15	1.7225 +35	1.36	3.3825 +15	1.2820 +36
.58	1.1221 +15	1.8709 +35	1.38	3.4536 +15	1.3246 +36
.60	1.1683 +15	2.0268 +35	1.40	3.5254 +15	1.3680 +36
.62	1.2150 +15	2.1874 +35	1.42	3.5979 +15	1.4122 +36
.64	1.2624 +15	2.3544 +35	1.44	3.6710 +15	1.4571 +36
.66	1.3103 +15	2.5287 +35	1.46	3.7449 +15	1.5029 +36
.68	1.3588 +15	2.7083 +35	1.48	3.8195 +15	1.5493 +36
.70	1.4079 +15	2.8934 +35	1.50	3.8948 +15	1.5966 +36
.72	1.4577 +15	3.0852 +35	1.52	3.9704 +15	1.6445 +36
.74	1.5080 +15	3.2841 +35	1.54	4.0471 +15	1.6930 +36
.76	1.5589 +15	3.4899 +35	1.56	4.1245 +15	1.7422 +36
.78	1.6105 +15	3.7033 +35	1.58	4.2026 +15	1.7921 +36
.80	1.6627 +15	3.9244 +35	1.60	4.2814 +15	1.8427 +36
.82	1.7154 +15	4.1527 +35	1.62	4.3609 +15	1.8941 +36

Table VII

Equation of state similar to case 1 but with universal coupling of all baryons ($x_H = 1$).

n (fm^{-3})	ρ (g/cm^3)	p ($dynes/cm^2$)	n (fm^{-3})	ρ (g/cm^3)	p ($dynes/cm^2$)
.04	6.7232 +13	1.6219 +32	.82	1.6983 +15	4.2542 +35
.06	1.0101 +14	4.8894 +32	.84	1.7516 +15	4.4992 +35
.08	1.3495 +14	1.1392 +33	.86	1.8055 +15	4.7512 +35
.10	1.6913 +14	2.2041 +33	.88	1.8601 +15	5.0111 +35
.12	2.0361 +14	3.7261 +33	.90	1.9154 +15	5.2780 +35
.14	2.3840 +14	5.6869 +33	.92	1.9714 +15	5.5528 +35
.16	2.7354 +14	8.1760 +33	.94	2.0280 +15	5.8301 +35
.18	3.0905 +14	1.0530 +34	.96	2.0853 +15	6.1118 +35
.20	3.4482 +14	1.2909 +34	.98	2.1432 +15	6.4005 +35
.22	3.8089 +14	1.5867 +34	1.00	2.2018 +15	6.6949 +35
.24	4.1727 +14	1.9458 +34	1.02	2.2612 +15	6.9975 +35
.26	4.5403 +14	2.3702 +34	1.04	2.3210 +15	7.3064 +35
.28	4.9122 +14	2.8654 +34	1.06	2.3816 +15	7.6226 +35
.30	5.2879 +14	3.4314 +34	1.08	2.4429 +15	7.9458 +35
.32	5.6682 +14	4.0711 +34	1.10	2.5048 +15	8.2740 +35
.34	6.0531 +14	4.7863 +34	1.12	2.5676 +15	8.6098 +35
.36	6.4429 +14	5.5790 +34	1.14	2.6307 +15	8.9504 +35
.38	6.8379 +14	6.4502 +34	1.16	2.6947 +15	9.2991 +35
.40	7.2386 +14	7.4016 +34	1.18	2.7593 +15	9.6549 +35
.42	7.6439 +14	8.4021 +34	1.20	2.8247 +15	1.0018 +36
.44	8.0555 +14	9.4477 +34	1.22	2.8907 +15	1.0388 +36
.46	8.4720 +14	1.0554 +35	1.24	2.9574 +15	1.0763 +36
.48	8.8942 +14	1.1729 +35	1.26	3.0246 +15	1.1143 +36
.50	9.3220 +14	1.2975 +35	1.28	3.0927 +15	1.1531 +36
.52	9.7551 +14	1.4293 +35	1.30	3.1614 +15	1.1925 +36
.54	1.0195 +15	1.5678 +35	1.32	3.2310 +15	1.2328 +36
.56	1.0640 +15	1.7110 +35	1.34	3.3009 +15	1.2735 +36
.58	1.1090 +15	1.8608 +35	1.36	3.3716 +15	1.3151 +36
.60	1.1547 +15	2.0183 +35	1.38	3.4433 +15	1.3576 +36
.62	1.2010 +15	2.1830 +35	1.40	3.5153 +15	1.4005 +36
.64	1.2479 +15	2.3555 +35	1.42	3.5880 +15	1.4441 +36
.66	1.2954 +15	2.5356 +35	1.44	3.6615 +15	1.4884 +36
.68	1.3435 +15	2.7237 +35	1.46	3.7358 +15	1.5334 +36
.70	1.3923 +15	2.9195 +35	1.48	3.8110 +15	1.5792 +36
.72	1.4417 +15	3.1234 +35	1.50	3.8863 +15	1.6254 +36
.74	1.4917 +15	3.3350 +35	1.52	3.9623 +15	1.6725 +36
.76	1.5423 +15	3.5544 +35	1.54	4.0390 +15	1.7201 +36
.78	1.5937 +15	3.7824 +35	1.56	4.1171 +15	1.7689 +36
.80	1.6457 +15	4.0154 +35	1.58	4.1956 +15	1.8180 +36

Table VIII

Star properties for case 1. The central baryon density n_c, star radius R, fractional red shift z, mass in solar masses $M/M_\odot$, moment of inertia I, total number of baryons A, fraction of baryons that are hyperons Y/A, and central energy density ρ_c.

n_c (fm^{-3})	R (km)	z	$M/M_\odot$	I ($g\ km^2$)	A	Y/A	ρ_c (g/cm^3)
.060			>.338		>1.066 +56		1.010 +14
.065	294.84	.0005	.094	3.857 +44	7.749 +55	0.	1.095 +14
.070	74.63	.0020	.103	1.113 +44	7.533 +55	0.	1.180 +14
.075	45.73	.0037	.115	1.107 +44	9.157 +55	0.	1.265 +14
.080	35.23	.0053	.126	1.193 +44	1.036 +56	0.	1.350 +14
.085	27.52	.0079	.145	1.379 +44	1.298 +56	0.	1.435 +14
.090	23.70	.0104	.164	1.590 +44	1.545 +56	0.	1.521 +14
.095	21.50	.0127	.182	1.809 +44	1.805 +56	0.	1.606 +14
.100	20.09	.0149	.199	2.026 +44	2.025 +56	0.	1.692 +14
.105	18.77	.0180	.223	2.337 +44	2.303 +56	0.	1.778 +14
.110	17.89	.0209	.245	2.651 +44	2.589 +56	0.	1.864 +14
.115	17.28	.0237	.267	2.963 +44	2.878 +56	0.	1.950 +14
.120	16.83	.0263	.288	3.267 +44	3.170 +56	0.	2.036 +14
.125	16.41	.0295	.314	3.650 +44	3.513 +56	0.	2.123 +14
.130	16.09	.0326	.338	4.028 +44	3.793 +56	0.	2.210 +14
.135	15.85	.0355	.362	4.397 +44	4.139 +56	0.	2.297 +14
.140	15.66	.0383	.384	4.752 +44	4.413 +56	0.	2.384 +14
.145	15.49	.0417	.411	5.189 +44	4.720 +56	0.	2.472 +14
.181	14.88	.0617	.569	7.836 +44	6.813 +56	0.	3.113 +14
.218	14.60	.0775	.685	9.736 +44	8.340 +56	0.	3.764 +14
.254	14.33	.0954	.808	1.159 +45	1.001 +57	0.	4.426 +14
.290	14.09	.1154	.936	1.342 +45	1.177 +57	0.	5.101 +14
.326	13.88	.1371	1.065	1.521 +45	1.355 +57	0.	5.789 +14
.363	13.69	.1599	1.190	1.688 +45	1.528 +57	0.	6.493 +14
.399	13.51	.1832	1.307	1.837 +45	1.697 +57	1.280 -05	7.214 +14
.435	13.37	.2032	1.400	1.946 +45	1.835 +57	4.964 -04	7.952 +14
.471	13.24	.2200	1.471	2.019 +45	1.945 +57	2.349 -03	8.706 +14
.508	13.11	.2352	1.529	2.067 +45	2.032 +57	5.962 -03	9.473 +14
.544	12.98	.2492	1.579	2.096 +45	2.106 +57	1.126 -02	1.026 +15
.580	12.85	.2625	1.621	2.109 +45	2.172 +57	1.800 -02	1.105 +15
.616	12.71	.2751	1.657	2.109 +45	2.229 +57	2.594 -02	1.186 +15
.653	12.58	.2869	1.688	2.100 +45	2.280 +57	3.480 -02	1.269 +15
.689	12.45	.2982	1.714	2.083 +45	2.316 +57	4.449 -02	1.353 +15
.725	12.32	.3089	1.737	2.060 +45	2.355 +57	5.448 -02	1.439 +15
.761	12.19	.3187	1.755	2.033 +45	2.386 +57	6.438 -02	1.526 +15
.798	12.07	.3278	1.769	2.004 +45	2.412 +57	7.428 -02	1.614 +15
.834	11.96	.3362	1.782	1.972 +45	2.433 +57	8.425 -02	1.704 +15
.870	11.85	.3442	1.791	1.939 +45	2.444 +57	9.454 -02	1.796 +15
.906	11.74	.3516	1.799	1.904 +45	2.459 +57	1.044 -01	1.889 +15
.943	11.64	.3582	1.805	1.871 +45	2.469 +57	1.138 -01	1.983 +15
.979	11.54	.3642	1.809	1.837 +45	2.476 +57	1.230 -01	2.079 +15
1.015	11.45	.3698	1.811	1.804 +45	2.481 +57	1.319 -01	2.176 +15
1.051	11.36	.3750	1.813	1.771 +45	2.484 +57	1.408 -01	2.274 +15

1.088	11.28	.3799	1.813	1.737 +45	2.485 +57	1.497 -01	2.374 +15
1.124	11.19	.3844	1.813	1.704 +45	2.485 +57	1.585 -01	2.475 +15
1.160	11.11	.3887	1.812	1.670 +45	2.483 +57	1.672 -01	2.577 +15
1.196	11.03	.3927	1.810	1.638 +45	2.479 +57	1.758 -01	2.681 +15

Table IX
Star properties for case 2.

n_c (fm^{-3})	R (km)	z	$M/M_\odot$	I ($g\ km^2$)	A	Y/A	ρ_c (g/cm^3)
.145	15.49	.0417	.411	5.190 +44	4.720 +56	0.	2.472 +14
.181	14.83	.0656	.599	8.377 +44	7.177 +56	0.	3.113 +14
.218	14.57	.0916	.793	1.184 +45	9.749 +56	0.	3.769 +14
.254	14.43	.1186	.982	1.524 +45	1.234 +57	0.	4.440 +14
.290	14.32	.1449	1.150	1.820 +45	1.470 +57	3.476 -05	5.128 +14
.326	14.23	.1647	1.266	2.011 +45	1.634 +57	1.163 -03	5.831 +14
.363	14.12	.1806	1.351	2.131 +45	1.755 +57	4.377 -03	6.547 +14
.399	14.00	.1944	1.418	2.205 +45	1.855 +57	9.863 -03	7.276 +14
.435	13.87	.2073	1.474	2.249 +45	1.936 +57	1.768 -02	8.018 +14
.471	13.72	.2195	1.522	2.268 +45	2.008 +57	2.742 -02	8.772 +14
.508	13.57	.2313	1.564	2.270 +45	2.072 +57	3.863 -02	9.539 +14
.544	13.41	.2427	1.600	2.258 +45	2.131 +57	5.093 -02	1.032 +15
.580	13.24	.2538	1.632	2.237 +45	2.175 +57	6.417 -02	1.111 +15
.616	13.08	.2646	1.659	2.208 +45	2.223 +57	7.770 -02	1.192 +15
.653	12.91	.2752	1.684	2.174 +45	2.258 +57	9.173 -02	1.275 +15
.689	12.75	.2854	1.705	2.136 +45	2.296 +57	1.054 -01	1.358 +15
.725	12.60	.2949	1.723	2.098 +45	2.321 +57	1.188 -01	1.444 +15
.761	12.46	.3038	1.737	2.059 +45	2.348 +57	1.313 -01	1.530 +15
.798	12.32	.3122	1.750	2.019 +45	2.365 +57	1.438 -01	1.618 +15
.834	12.19	.3203	1.760	1.978 +45	2.385 +57	1.557 -01	1.708 +15
.870	12.06	.3280	1.768	1.936 +45	2.401 +57	1.674 -01	1.799 +15
.906	11.93	.3353	1.775	1.895 +45	2.408 +57	1.792 -01	1.891 +15
.943	11.82	.3420	1.780	1.855 +45	2.419 +57	1.896 -01	1.985 +15
.979	11.71	.3482	1.783	1.817 +45	2.427 +57	1.997 -01	2.081 +15
1.015	11.60	.3539	1.786	1.780 +45	2.432 +57	2.093 -01	2.177 +15
1.051	11.50	.3595	1.787	1.742 +45	2.429 +57	2.195 -01	2.275 +15
1.088	11.40	.3646	1.788	1.705 +45	2.431 +57	2.288 -01	2.375 +15
1.124	11.30	.3696	1.787	1.669 +45	2.432 +57	2.379 -01	2.475 +15
1.160	11.21	.3743	1.786	1.633 +45	2.431 +57	2.467 -01	2.577 +15
1.196	11.12	.3787	1.784	1.598 +45	2.429 +57	2.555 -01	2.681 +15

Table X
Star properties for case 3.

n_c (fm^{-3})	R (km)	z	$M/M_\odot$	I ($g\ km^2$)	A	Y/A	ρ_c (g/cm^3)
.145	15.49	.0417	.411	5.189 +44	4.720 +56	0.	2.472 +14
.181	14.83	.0656	.599	8.377 +44	7.177 +56	0.	3.113 +14
.218	14.57	.0916	.793	1.184 +45	9.749 +56	0.	3.769 +14
.254	14.43	.1186	.982	1.524 +45	1.234 +57	0.	4.440 +14
.290	14.32	.1461	1.157	1.833 +45	1.480 +57	0.	5.128 +14
.326	14.21	.1713	1.304	2.078 +45	1.685 +57	1.772 -04	5.833 +14
.363	14.10	.1905	1.406	2.231 +45	1.838 +57	2.018 -03	6.555 +14
.399	13.98	.2084	1.492	2.339 +45	1.958 +57	6.665 -03	7.291 +14
.435	13.84	.2257	1.567	2.410 +45	2.075 +57	1.391 -02	8.043 +14
.471	13.68	.2426	1.632	2.454 +45	2.175 +57	2.323 -02	8.812 +14
.508	13.51	.2591	1.689	2.476 +45	2.265 +57	3.398 -02	9.598 +14
.544	13.34	.2752	1.740	2.480 +45	2.339 +57	4.581 -02	1.040 +15
.580	13.17	.2909	1.784	2.470 +45	2.413 +57	5.796 -02	1.122 +15
.616	13.00	.3061	1.822	2.451 +45	2.471 +57	7.041 -02	1.206 +15
.653	12.84	.3204	1.854	2.423 +45	2.527 +57	8.232 -02	1.292 +15
.689	12.68	.3340	1.880	2.390 +45	2.568 +57	9.409 -02	1.380 +15
.725	12.52	.3468	1.903	2.352 +45	2.602 +57	1.055 -01	1.470 +15
.761	12.37	.3589	1.921	2.310 +45	2.638 +57	1.162 -01	1.562 +15
.798	12.23	.3704	1.936	2.266 +45	2.660 +57	1.270 -01	1.656 +15
.834	12.09	.3814	1.948	2.219 +45	2.685 +57	1.370 -01	1.752 +15
.870	11.95	.3917	1.958	2.172 +45	2.697 +57	1.471 -01	1.850 +15
.906	11.83	.4011	1.965	2.125 +45	2.713 +57	1.561 -01	1.951 +15
.943	11.71	.4100	1.970	2.079 +45	2.725 +57	1.648 -01	2.053 +15
.979	11.59	.4182	1.973	2.032 +45	2.726 +57	1.736 -01	2.157 +15
1.015	11.48	.4260	1.975	1.986 +45	2.732 +57	1.818 -01	2.263 +15
1.051	11.36	.4334	1.975	1.940 +45	2.735 +57	1.897 -01	2.372 +15
1.088	11.26	.4403	1.974	1.894 +45	2.735 +57	1.974 -01	2.482 +15
1.124	11.15	.4468	1.973	1.849 +45	2.734 +57	2.049 -01	2.595 +15
1.160	11.05	.4529	1.970	1.806 +45	2.724 +57	2.126 -01	2.710 +15
1.196	10.96	.4586	1.966	1.763 +45	2.719 +57	2.197 -01	2.827 +15

Table XI
Star properties for a case like 1 with universal coupling for baryons ($x_H = 1$).

n_c (fm^{-3})	R (km)	z	$M/M_\odot$	I (g km^2)	A	Y/A	ρ_c (g/cm^3)
.145	15.49	.0417	.411	5.189 +44	4.720 +56	0.	2.472 +14
.181	14.88	.0618	.569	7.837 +44	6.813 +56	0.	3.113 +14
.218	14.60	.0775	.685	9.736 +44	8.339 +56	0.	3.764 +14
.254	14.33	.0954	.808	1.159 +45	1.000 +57	0.	4.426 +14
.290	14.09	.1154	.936	1.342 +45	1.177 +57	0.	5.101 +14
.326	13.88	.1371	1.065	1.521 +45	1.355 +57	0.	5.789 +14
.363	13.69	.1599	1.190	1.688 +45	1.528 +57	0.	6.493 +14
.399	13.51	.1834	1.308	1.838 +45	1.698 +57	0.	7.214 +14
.435	13.35	.2060	1.412	1.962 +45	1.854 +57	1.657 -04	7.953 +14
.471	13.19	.2275	1.503	2.058 +45	1.986 +57	1.089 -03	8.710 +14
.508	13.04	.2481	1.581	2.130 +45	2.112 +57	3.005 -03	9.486 +14
.544	12.89	.2678	1.649	2.181 +45	2.217 +57	5.842 -03	1.028 +15
.580	12.75	.2862	1.707	2.213 +45	2.309 +57	9.470 -03	1.109 +15
.616	12.60	.3039	1.757	2.229 +45	2.382 +57	1.393 -02	1.192 +15
.653	12.46	.3207	1.800	2.233 +45	2.454 +57	1.900 -02	1.278 +15
.689	12.31	.3367	1.836	2.225 +45	2.515 +57	2.455 -02	1.365 +15
.725	12.18	.3518	1.867	2.210 +45	2.561 +57	3.052 -02	1.454 +15
.761	12.04	.3661	1.892	2.187 +45	2.608 +57	3.661 -02	1.546 +15
.798	11.91	.3798	1.914	2.159 +45	2.647 +57	4.279 -02	1.639 +15
.834	11.78	.3924	1.931	2.127 +45	2.672 +57	4.905 -02	1.735 +15
.870	11.66	.4042	1.945	2.092 +45	2.699 +57	5.517 -02	1.833 +15
.906	11.54	.4152	1.956	2.055 +45	2.721 +57	6.127 -02	1.933 +15
.943	11.42	.4255	1.965	2.017 +45	2.738 +57	6.727 -02	2.035 +15
.979	11.31	.4351	1.971	1.979 +45	2.743 +57	7.333 -02	2.140 +15
1.015	11.21	.4438	1.975	1.939 +45	2.752 +57	7.918 -02	2.247 +15
1.051	11.11	.4521	1.977	1.900 +45	2.758 +57	8.499 -02	2.355 +15
1.088	11.01	.4597	1.978	1.860 +45	2.761 +57	9.074 -02	2.466 +15
1.124	10.92	.4668	1.978	1.821 +45	2.762 +57	9.642 -02	2.580 +15
1.160	10.82	.4734	1.977	1.782 +45	2.760 +57	1.020 -01	2.695 +15
1.196	10.74	.4795	1.975	1.744 +45	2.757 +57	1.076 -01	2.813 +15

Footnotes and References

1. M.H. Johnson and E. Teller, Phys. Rev. **98**, 783 (1955); H.P. Duerr, Phys. Rev. **103**, 469 (1956).
2. J.D. Walecka, Ann. of Phys. (N.Y.) **83**, 491 (1974); S.A. Chin, Ann. of Phys. **108**, 301 (1977); S.A. Chin and J.D. Walecka, Phys. Lett. **52B**, 24 (1974).
3. J. Boguta and A.R. Bodmer, Nucl. Phys. **A292**, 413 (1977); J. Boguta and J. Rafelski, Phys. Lett. **71B**, 22 (1977).
4. J. Boguta and H. Stocker, Phys. Lett. **120B**, 289 (1983).
5. B.D. Serot and J.D. Walecka, Phys. Lett. **87B**, 172 (1980); C.J. Horowitz and B.D. Serot, Nucl. Phys. **A368**, 503 (1981).
6. J. Boguta, Phys. Lett. **B106**, 245 (1981); Phys. Lett. **B106**, 250 (1981); Nucl. Phys. **A372**, 386 (1981).
7. B. Banerjee, N.K. Glendenning and M. Gyulassy, Nucl. Phys. **A361**, 326 (1981).
8. N.K. Glendenning, B. Banerjee, and M. Gyulassy, Ann. of Phys. **149**, 1 (1983).
9. N.K. Glendenning, P. Hecking, and V. Ruck, Ann. of Phys. **149**, 22 (1983).
10. N.K. Glendenning, Phys. Lett. **114B**, 392 (1982).
11. S.I.A. Garpman, N.K. Glendenning and Y.J. Karant, Nucl. Phys. **A322**, 382 (1979); N.K. Glendenning, Phys. Rev. **C23**, 2757 (1981).
12. V.A. Ambartsumyan and G.S. Saakyan, Sov. Astron. **4**, 187 (1960).
13. L.M. Libby and F.J. Thomas, Phys. Lett. **B30**, 88 (1969); W.D. Langer and L.C. Rosen, Astrophys. Space Sci. **6**, 217 (1970); V.R. Pandharipande and V.K. Garde, Phys. Lett. **B39**, 608 (1972).
14. V.R. Pandharipande, Nucl. Phys. **A178**, 123 (1971).
15. H.A. Bethe and M. Johnson, Nucl. Phys. **A230**, 1 (1974).
16. S.A. Moszkowski, Phys. Rev. **D9**, 1613 (1974).
17. S.-H. Gas, Y.-Z. Ge, Y.C. Leung, Z.-W. Li and S.-R. Liang, Astrophs. J. **245**, 1110 (1981).
18. For reviews see G. Baym, Les Houches 1977 Session XXX ed. by Balian, Rho, and Ripka (North Holland, Amsterdam, 1978), vol. 2, p. 748; D.K. Campbell, loc. cit., p. 549; R.F. Sawyer, loc. cit., p. 717; A.B. Migdal, Rev. Mod. Phys. **50**, 107 (1978).
19. We use the notation of J.D. Bjorken and S.D. Drell, **Relativistic Quantum Mechanics** (1964) and **Relativistic Quantum Fields** (1965) (McGraw Hill, New York).
20. W.D. Myers, Droplet Model of Atomic Nuclei (Plenum, New York, 1977).
21. A.B. Migdal, Rev. Mod. Phys. **50**, 107 (1978); J.M. Irvine and I.R. Rogers, J. Phys. **G3**, 1699 (1977); G.E. Brown and W. Weise, Phys. Reports **27**, 1 (1976).
22. Ya B. Zel'dovich, JETP (Soviet Phys.) **14**, 1143 (1962).
23. S. Weinberg, **Gravitation and Cosmology**, John Wiley and Sons, N.Y. 1972.
24. J.W. Negele and D. Vautherin, Nucl. Phys. **A207**, 298 (1973).
25. B.K. Harrison and J.A. Wheeler as quoted by B.K. Harrison et. al. in **Gravitation Theory and Gravitational Collapse**, (University of Chicago Press (1965)).
26. R.N. Manchester and J.H. Taylor, **Pulsars**, (W.H. Freeman and Co., San Francisco, (1977)).
27. H. Bondi, Proc. Roy. Soc. (London) **A281**, 39 (1964).

28. R. Ruffini in **Physics and Astrophysics of Neutron Stars and Black Holes** (North Holland Publ. Co. 1978) p. 287.

29. V. Canuto in **Physics and Astrophysics of Neutron Stars and Black Holes** (North Holland Publ. Co. 1978) p. 449.

30. C. Rhoades and R. Ruffini, Phys. Rev. Lett. **32** 1324 (1974).

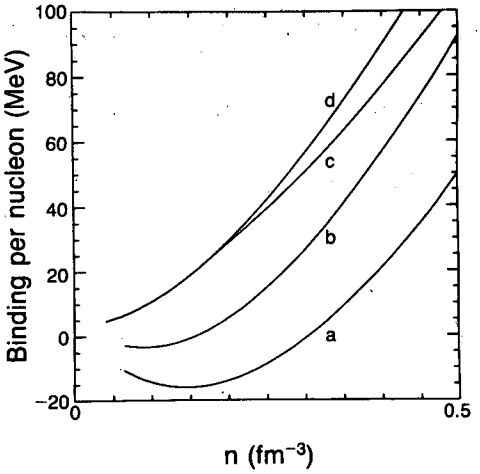

Figure 1 XBL 8311-3418

Fig. 1. Binding energy per nucleon, $\rho/n - m_n$, as a function of baryon number density, n, for (a) symmetric nuclear matter, (b) pure neutron matter, (c) the present theory of neutron star matter including hyperons and free π^- condensate and with a ρ-meson coupling that yields the correct charge symmetry energy in nuclear matter, (d) like (c) but without hyperons and π condensate.

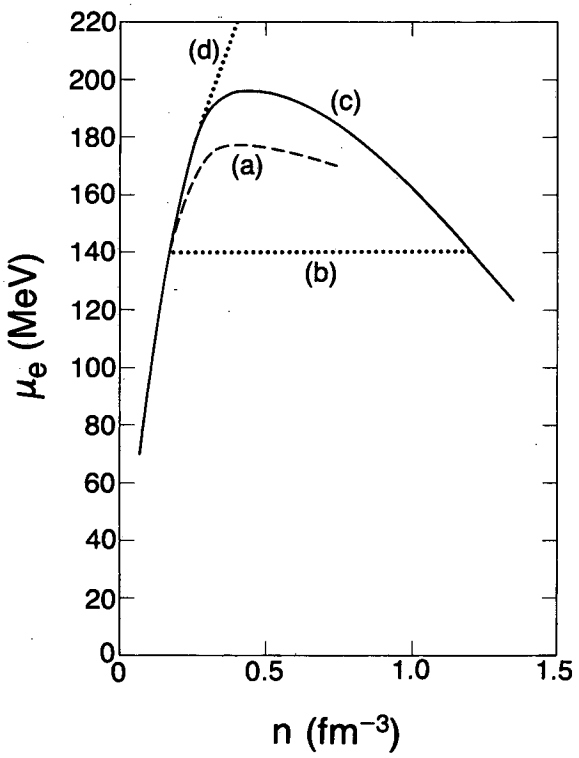

Figure 2 XBL 8311-3427

Fig. 2. Electron chemical potential as a function of baryon number density in neutron star matter showing quenching for (a) interacting pion condensate in β-stable neutron-proton matter with correct charge symmetry energy (from ref. 9), (b) free pion condensate in stable matter containing nucleons and hyperons and with correct charge symmetry energy (c) like (b) but no pion condensate (d) no hyperons or condensate but correct charge symmetry energy.

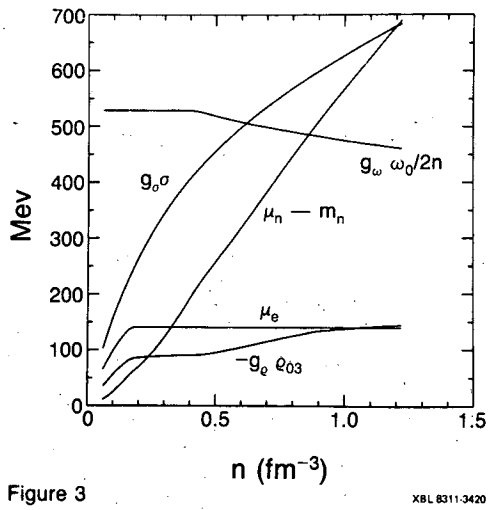

Figure 3

XBL 8311-3420

Fig. 3. The σ, ω_0 and ρ field strengths and the two chemical potentials as a function of baryon number density for our theory (case 1). The coupling constants refer to the nucleon. For hyperon coupling, refer to Eq. (58). The electron chemical potential saturates at m_π because of a free π^- Bose condensate.

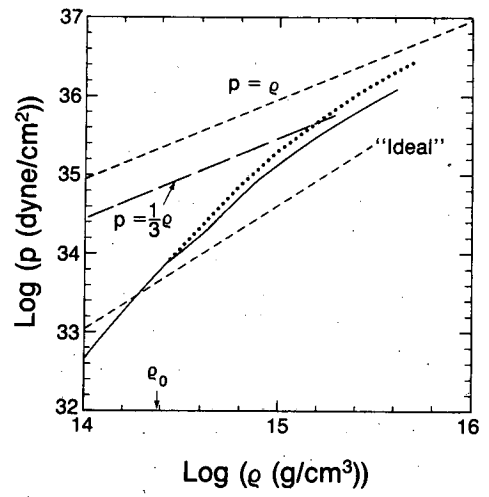

Figure 4

XBL 8311-3431

Fig. 4. Equation of state p vs. ρ for case 1 with nucleons, hyperons, isobars and π^- condensate (solid line) is compared with case 5, for which hyperons, isobars and condensate are absent (dotted line). In both, the charge symmetry energy is correct for nuclear matter. Other curves show the causal limit ($p=\rho$), the ideal ultrarelativistic gas ($p=\rho/3$) and an ideal neutron gas. The density of ordinary nuclear matter is marked. At ultra high density our theory approaches the causal limit.

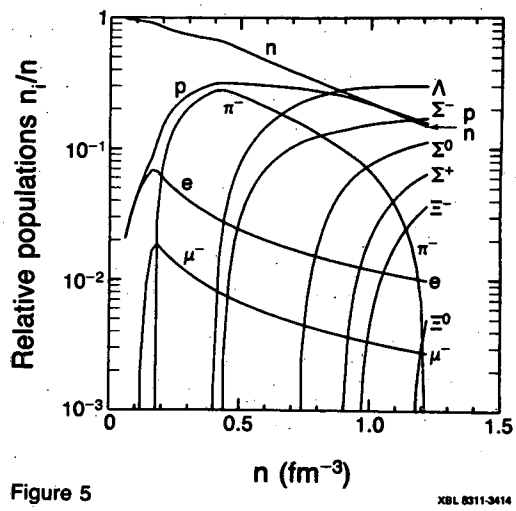

Figure 5

Fig. 5. Relative populations as a function of baryon density for our theory (case 1). In the pion condensate region, $0.18 < n < 1.22$ fm^{-3}, the lepton number densities are constant (decreasing relative populations). The π condensate is ultimately quenched by the hyperon populations. Hyperons appear in the order $\Lambda,\Sigma^-,\Sigma^0,\Sigma^+,\Xi^-,\Xi^0$. The Δ's do not appear in this density range.

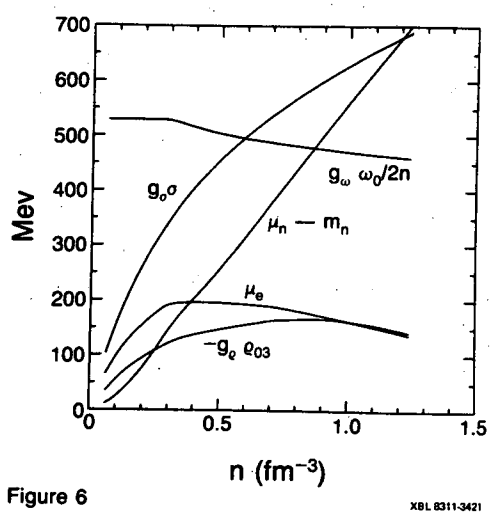

Figure 6

Fig. 6. Field strengths and chemical potentials for case 2. The electron chemical potential is quenched by the hyperons in this case where the pion is assumed to have a repulsive self-energy which prevents its condensation.

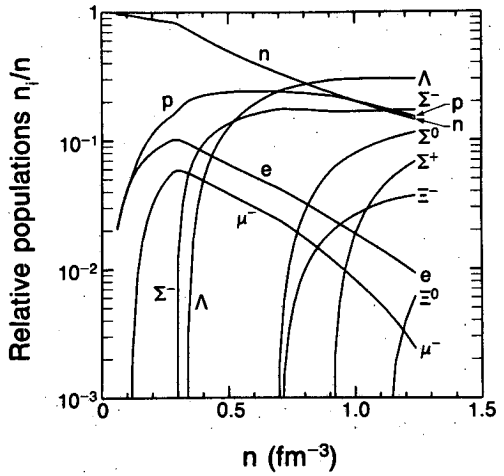

Figure 7

XBL 8311-3422

Fig. 7. Relative populations for case 2, where pions do not condense. Lepton populations reach higher levels than case 1 but nevertheless are quenched by hyperons. The hyperons have lower thresholds when pions do not condense.

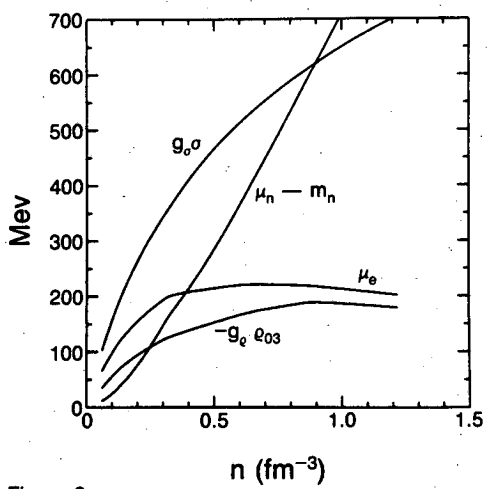

Figure 8

XBL 8311-3430

Fig. 8. Field strengths σ, ρ and chemical potentials for case 3 where nucleons, hyperons and isobars are universally coupled. In this case of universal coupling, ω_0 is proportional to n.

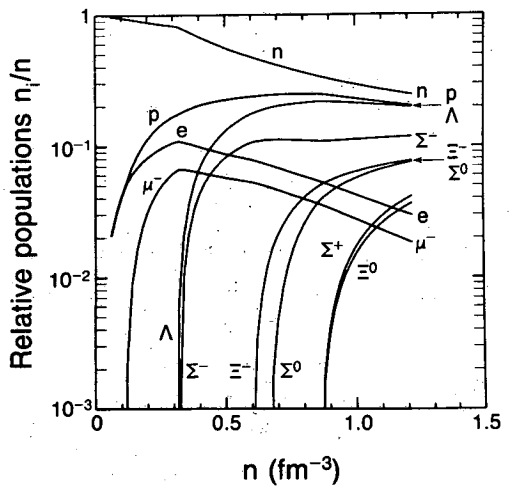

Fig. 9. Populations in case all baryons are universally coupled, and pions do not condense by reason of an assumed repulsive self-energy (case 3).

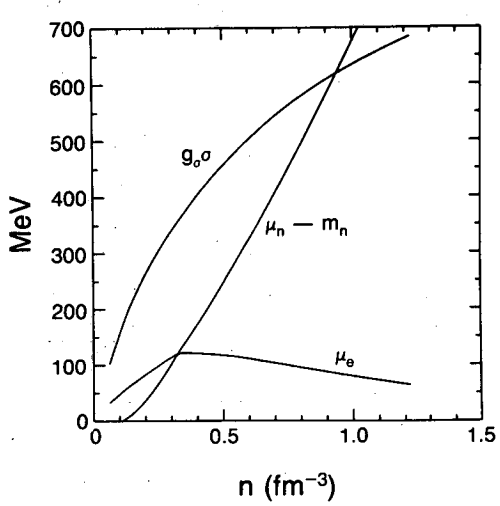

Fig. 10. Field strengths and chemical potentials for case 4. Here the ρ coupling, g_ρ=0 and all baryons are universally coupled.

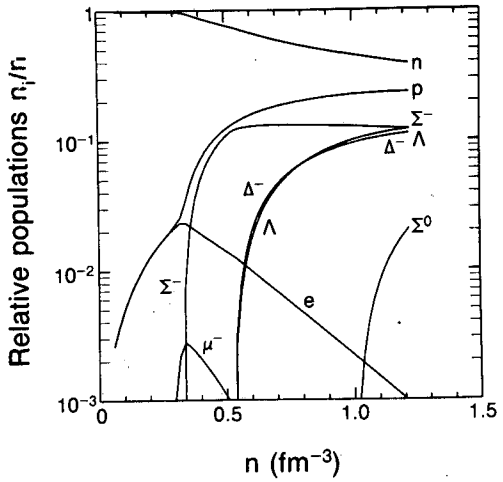

Figure 11 XBL 8311-3415

Fig. 11. Relative populations for case 4, where all baryons are universally coupled and g_ρ=0. In this case the charge symmetry energy derives only from the difference in neutron and proton kinetic energies and is too small compared to the empirical value. Populations are radically different from preceeding cases. The protons are less populous because of the smaller symmetry energy, and for the same reason the Σ^- makes an early appearance, quenching the leptons.

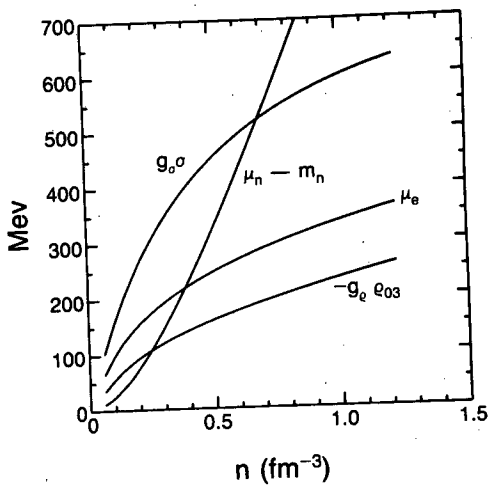

Figure 12 XBL 8311-3413

Fig. 12. Field strengths and chemical potentials for case 5 where hyperons, isobars and pions are absent in the theory. Charge symmetry energy for nuclear matter is correct.

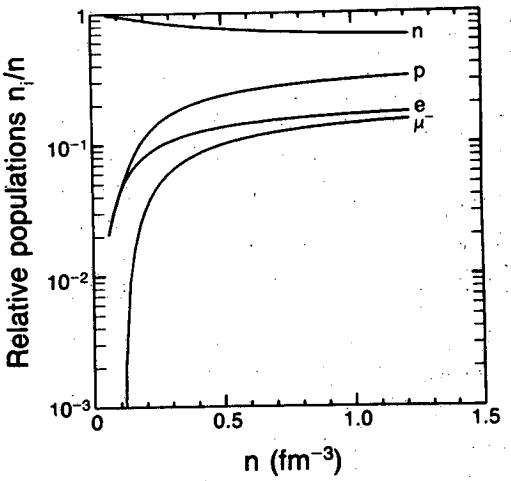

Figure 13

XBL 8311-3409

Fig. 13. Relative populations in the absence of hyperons, isobars and pions in the theory, (case 5) but with correct symmetry energy.

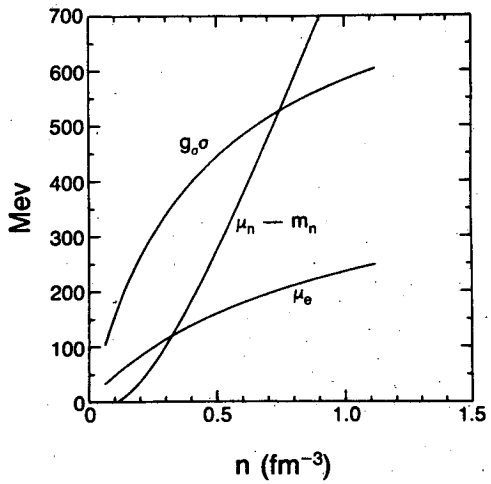

Figure 14

XBL 8311-3419

Fig. 14. Field strength σ and chemical potentials for case 6 where hyperons, isobars and pions are absent and $g_\rho = 0$.

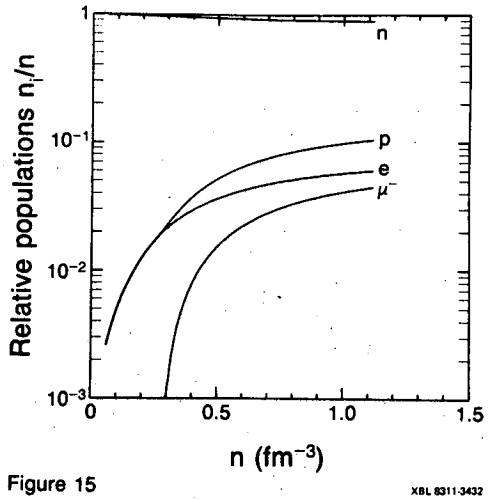

Figure 15

XBL 8311-3432

Fig. 15. Relative populations for case 6 where hyperons, isobars and pions are absent from the theory and $g_\rho = 0$. Therefore charge symmetry energy is too small and proton population is consequently smaller than for case 5.

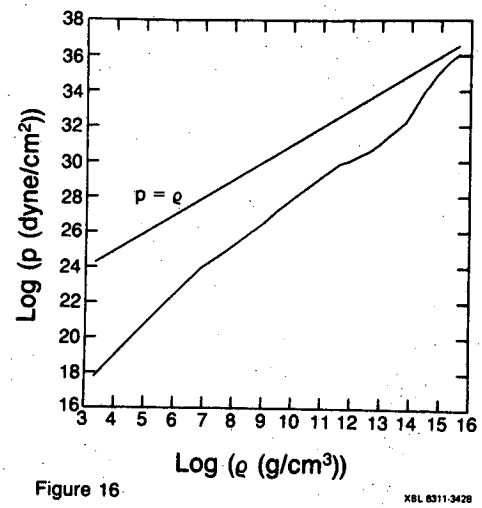

Figure 16

XBL 8311-3428

Fig. 16. Equation of state over wide density range appearing in neutron stars from the crust to the inner core. Region III ($\rho > 2 \times 10^{13}$ g/cm^3) is the hadronic gas region of the core (this work), II is the neutron rich metallic lattice region (Negele and Vautherin[24]) and I ($\rho < 10^{11}$ g/cm^3) is the Coulomb lattice region (Harrison and Wheeler[25]).

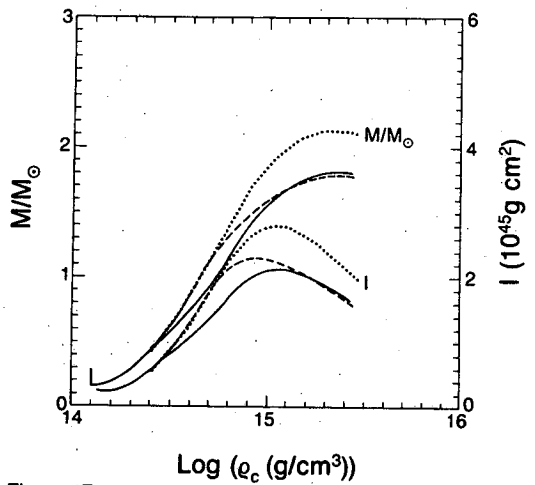

Fig. 17. Mass in solar masses and moment of inertia of neutron stars as a function of central density for case 1 (solid lines) with hyperons and π^- condensate, for case 2 (dashed lines) where condensate is absent and case 5 (dots) where both hyperons and condensate are absent. Charge symmetry energy is correct in all cases for nuclear matter. Beyond the maximum in the mass the star is unstable to gravitational collapse. The lower mass limit in the theory is about 0.09 solar masses. Below the corresponding central density until the white dwarf region, hydrostatic equilibrium is lost.

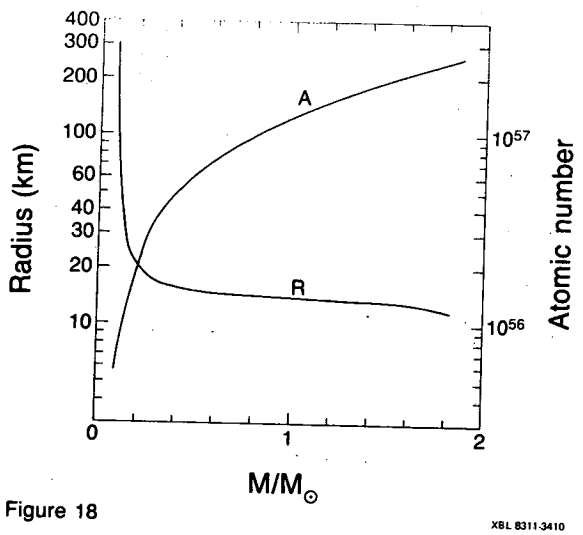

Fig. 18. Neutron star radius as a function of its mass. Stars near the lower limit of stability have very large radii. The atomic number A (total baryon number) is also shown.

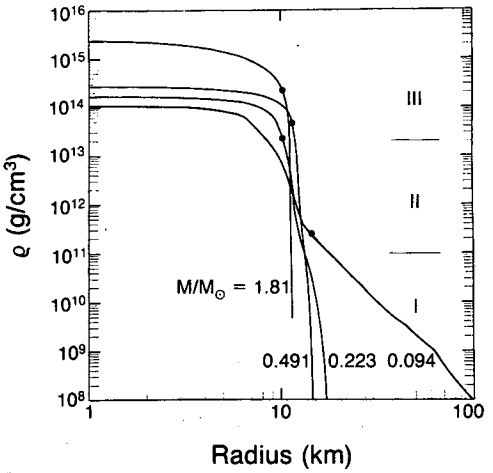

Figure 19 XBL 8311-3433

Fig. 19. Neutron star density as a function of the Schwarzchild radial coordinate for the two limiting neutron star configurations in our theory and two intermediate ones. The edge is very sharp for all stars except those very close to the lower stability limit of the central density. The three density ranges are those of Table III and Fig. 16. The circle on each curve marks the point interior to which 95% of the stars mass is contained.

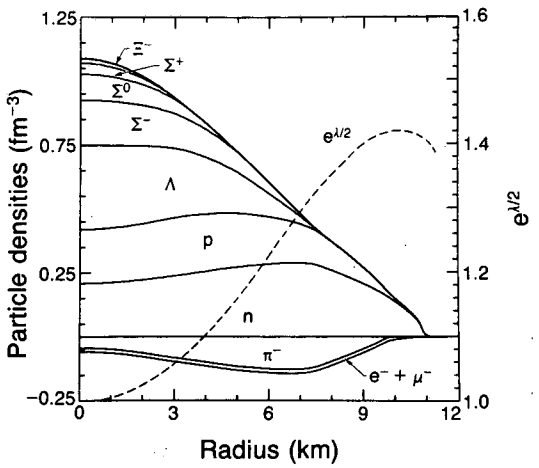

Figure 20 XBL 8311-3417

Fig. 20. Onion skin depiction for case 1 of the composition of the most massive star in our theory (1.82 $M_\odot$) as a function of Schwarzchild radial coordinate. Central baryon number density is 1.088 fm^{-3}. Baryons are plotted (cumulatively) above the axis, and pions and leptons below. The core is dominated by hyperons. Leptons have a small constant density throughout the region where pions are condensed. The dashed line shows the Schwarzchild radial metric function which relates the proper number densities at different radii (cf. eq. 58).

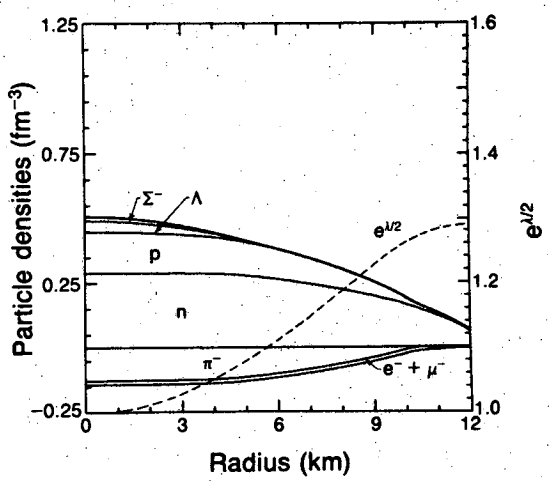

Figure 21

XBL 8311-3411

Fig. 21. As in Fig. 20 but for a star having central baryon number density 0.508 fm^{-3} and a mass 1.53 $M_\odot$.

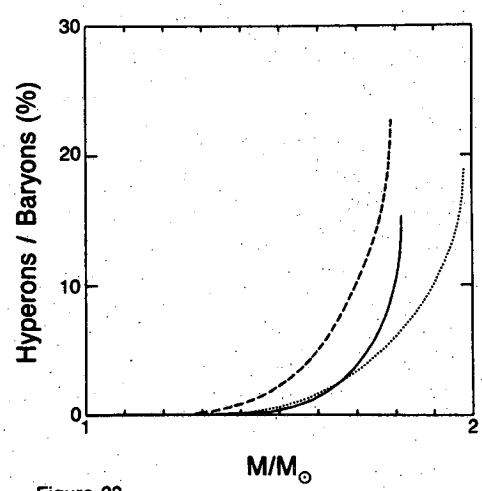

Figure 22

XBL 8311-3429

Fig. 22. Hyperon fraction of neutron stars as a function of mass for case 1. The fraction rises very rapidly as the limit of gravitational stability is reached. Solid line is for case 1 where free pions condense, dashed line is for case 2 where pions are not admitted and dotted line is for case 3 where the baryons are universally coupled and pions condensate is not admitted.

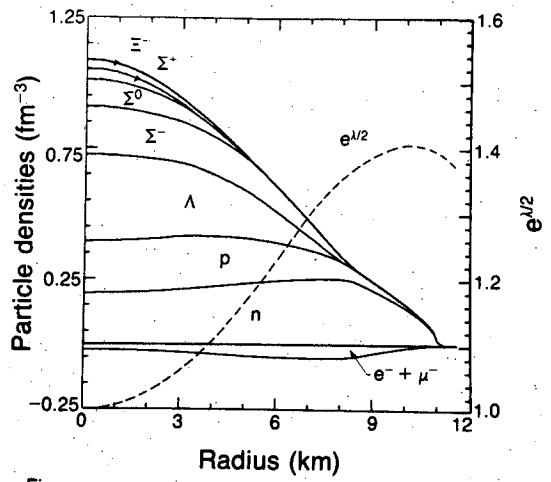

Figure 23

XBL 8311-3434

Fig. 23. Composition of star having central baryon number of 1.088 fm^{-3} as in Fig. 21 and mass 1.79 $M_\odot$ but for the case 2 in which pions are not admitted as for example because of a repulsive self-energy.

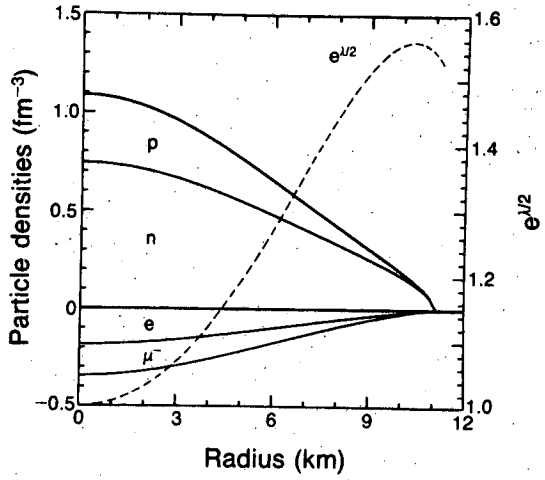

Figure 24

XBL 8311-3416

Fig. 24. Composition of star having central baryon density of 1.088 fm^{-3} as in Fig. 21, and mass 2.14 $M_\odot$ in which hyperons, isobars and pion condensate are omitted from the theory (case 5). In contrast to Figs. 20 and Fig. 23 there are large lepton populations.

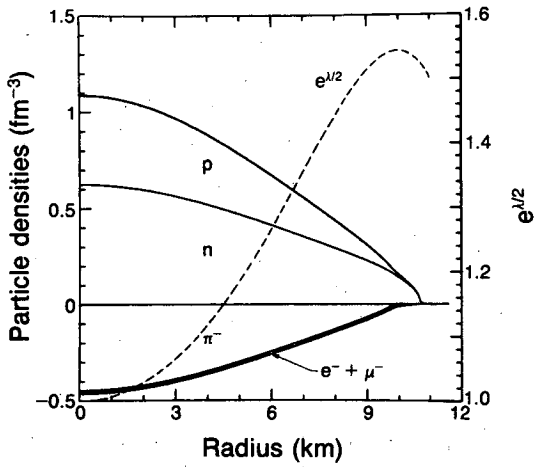

Figure 25

XBL 8311-3423

Fig. 25. Composition as in Fig. 20 of star having central baryon density of 1.088 fm^{-3} and mass 2.04 $M_\odot$, in which hyperons and isobars are omitted from the theory, but in which free pions condense (case 7).

TECHNICAL INFORMATION DEPARTMENT
LAWRENCE BERKELEY LABORATORY
UNIVERSITY OF CALIFORNIA
BERKELEY, CALIFORNIA 94720